Econometrica, Vol. 89, No. 5 (September, 2021), 2375–2408

USING THE SEQUENCE-SPACE JACOBIAN TO SOLVE AND ESTIMATE HETEROGENEOUS-AGENT MODELS

ADRIEN AUCLERT
Department of Economics, Stanford University, CEPR, and NBER

BENCE BARDÓCZY
Federal Reserve Board of Governors

MATTHEW ROGNLIE
Department of Economics, Northwestern University and NBER

LUDWIG STRAUB
Department of Economics, Harvard University and NBER

We propose a general and highly efficient method for solving and estimating general equilibrium heterogeneous-agent models with aggregate shocks in discrete time. Our approach relies on the rapid computation of *sequence-space Jacobians*—the derivatives of perfect-foresight equilibrium mappings between aggregate sequences around the steady state. Our main contribution is a fast algorithm for calculating Jacobians for a large class of heterogeneous-agent problems. We combine this algorithm with a systematic approach to composing and inverting Jacobians to solve for general equilibrium impulse responses. We obtain a rapid procedure for likelihood-based estimation and computation of nonlinear perfect-foresight transitions. We apply our methods to three canonical heterogeneous-agent models: a neoclassical model, a New Keynesian model with one asset, and a New Keynesian model with two assets.

KEYWORDS: Computational methods, general equilibrium, heterogeneous agents, linearization.

1. INTRODUCTION

A RAPIDLY EXPANDING LITERATURE in macroeconomics incorporates rich heterogeneity into dynamic general equilibrium models. A central challenge in this literature is that equilibrium involves the time-varying, high-dimensional distribution of agents over their state variables.

In this paper, we propose a general, systematic, and highly efficient method to deal with this challenge. Our method follows Reiter (2009) by perturbing the model to first order in aggregates. But, while the Reiter method writes equilibrium as a system of linear equations in the *state space*, we instead write it as a system of linear equations in the space of perfect-foresight sequences—the *sequence space*. Since the size of this system is independent of the size of the state space, it becomes feasible to solve and estimate models

Adrien Auclert: aauclert@stanford.edu
Bence Bardóczy: bence.a.bardoczy@frb.gov
Matthew Rognlie: matthew.rognlie@northwestern.edu
Ludwig Straub: ludwigstraub@fas.harvard.edu

For helpful comments, we thank four anonymous referees, as well as Riccardo Bianchi-Vimercati, Luigi Bocola, Michael Cai, Jesus Fernández-Villaverde, Joao Guerreiro, Kurt Mitman, Ben Moll, Laura Murphy, Martin Souchier, and Christian Wolf. Martin Souchier also provided outstanding research assistance. This research is supported by National Science Foundation Grant SES-1851717. This paper reflects our personal views and does not necessarily represent those of the Federal Reserve Board or the Federal Reserve System.

 https://doi.org/10.3982/ECTA17434

that feature very rich heterogeneity. Our sequence-space approach builds on Boppart, Krusell, and Mitman (2018), who solved for nonlinear impulse responses to small shocks, but we obtain a much faster solution by directly exploiting linearity.

We demonstrate the power of our method by solving and estimating three models, with increasing degrees of complexity, at unparalleled speed. A code repository accompanies this paper and provides general-purpose routines that automate the new algorithms we introduce.[1]

The central objects in our method are *sequence-space Jacobians*: the derivatives of equilibrium mappings between aggregate sequences around the steady state. These Jacobians summarize every aspect of the model that is relevant for general equilibrium. For example, consider a standard incomplete markets model. That model features a Jacobian $\mathcal{J}^{C,r}$ that maps, to first order, changes in the sequence of real interest rates $\{r_t\}$ to changes in the sequence of aggregate consumption $\{C_t\}$. Under the hood, this mapping includes the heterogeneous responses of households to changes in r, as well as the evolution of the distribution of agents over time that it induces. But to know the aggregate effect of r on C, all we need to know is $\mathcal{J}^{C,r}$: it is a *sufficient statistic*. Our method exploits this property. We compute all relevant sequence-space Jacobians, and then compose and invert these Jacobians to obtain the model's full set of impulse responses.

Our main contribution is a fast algorithm for computing Jacobians for a large class of heterogeneous-agent problems, truncated to a horizon of $T \times T$. A direct approach to calculating these Jacobians is quite costly. For instance, calculating column s of $\mathcal{J}^{C,r}$, the response to a shock to r_s, requires iterating backward to obtain the consumption policy at each date, then iterating forward to obtain the distribution at each date. The direct approach repeats this procedure for each column $s = 0, \ldots, T-1$. Our method, by contrast, exploits the structure of the linearized heterogeneous-agent problem around the steady state, which we capture formally in Proposition 1. It requires only a single backward iteration from $T-1$ to obtain the consumption policy and impulses to the distribution. These objects are then efficiently combined with information from the steady-state solution to form the full Jacobian, lowering the cost by a factor of about T relative to the direct approach. Our algorithm therefore provides a dramatic speed improvement, since T is typically equal to at least 300 in practice, and sometimes as large as 1000.

We combine this algorithm with a systematic approach to composing and inverting Jacobians to solve for general equilibrium impulse responses. Equilibrium in the sequence space can always be expressed as a solution to a nonlinear system

$$\mathbf{F}(\mathbf{X}, \mathbf{Z}) = 0, \tag{1}$$

where $\mathbf{X}$ represents the time path of endogenous variables (usually aggregate prices and quantities) and $\mathbf{Z}$ represents the time path of exogenous shocks. Obtaining the impulse responses of unknowns to shocks, $d\mathbf{X} = -\mathbf{F}_{\mathbf{X}}^{-1}\mathbf{F}_{\mathbf{Z}}\, d\mathbf{Z}$, requires computing the Jacobians $\mathbf{F}_{\mathbf{X}}$ and $\mathbf{F}_{\mathbf{Z}}$, which are formed by combining Jacobians from different parts of the model. Starting from the heterogeneous-agent Jacobians computed using our fast algorithm, this can be achieved by any method that systematically applies the chain rule. We propose one such method, forward accumulation along a directed acyclic graph (DAG). This procedure can be automated, and it usually only takes a few milliseconds.

[1] See https://github.com/shade-econ/sequence-jacobian, which provides routines written in Python, as well as pedagogical notebooks. A separate replication archive (https://github.com/shade-econ/ssj-replication) uses these routines to produce all figures and tables presented in this paper.

We verify that our method is accurate by showing that it delivers exactly the same solution as the Reiter method, for models where the Reiter method is feasible. Like all perturbation methods, both our method and the Reiter method are subject to error in taking derivatives; to allow for a precise comparison, we therefore use automatic differentiation to take error-free derivatives in both methods. We then demonstrate accuracy in two ways. First, we show that in response to specific 1% shocks, impulse responses under the two methods differ everywhere by less than 10^{-9}%. Second, we provide a method to recover the state-space law of motion from our sequence-space solution, and show that matrices in this law of motion differ from the same matrices obtained using the Reiter method by a maximum of less than 10^{-8}. With accuracy established, we additionally discuss how varying the truncation horizon T, or replacing automatic with numerical differentiation, can affect these errors.

In sum, our method enables researchers to obtain model Jacobians and linearized general equilibrium impulse responses, accurately and rapidly, in models with heterogeneous agents that can potentially be very complex. To show how these objects can be used in practice, we cover two applications that are very common in applied research: estimation on time-series data, and computation of nonlinear perfect-foresight transitions.

To build toward estimation, we first summarize the Boppart, Krusell, and Mitman (2018) simulation procedure. As they pointed out, the linearized impulse responses to shocks truncated to a horizon of T form an MA($T-1$) representation of the model with aggregate shocks, which yields a straightforward simulation procedure. These sample paths can be used to calculate approximate time-series moments, which in principle can then be used for estimation.

We next provide an alternative route, which is to use analytical formulas to calculate the model's time-series moments directly from impulse responses. From here, we can directly compute the likelihood function of any empirical time series. Given a prior over parameters, we can then find the posterior mode and trace out the posterior distribution via Markov chain Monte Carlo methods. Here, a critical benefit of our sequence-space method is that it makes it easy to reuse Jacobians, especially heterogeneous-agent Jacobians, across multiple computations of the likelihood function. This dramatically speeds up estimation, especially for the parameters of shock processes, and also for model parameters that do not affect the steady state.

Finally, we demonstrate how to solve equation (1) nonlinearly by using our sequence-space Jacobians in a quasi-Newton method. We consider two types of nonlinear transitions: large temporary shocks, and transitions to a new steady state. We show how, for the examples we consider, sequence-space Jacobians allow convergence to the nonlinear solution in just a few iterations.

Throughout the paper, we apply our methods to three canonical heterogeneous-household models of increasing complexity: a neoclassical model in the spirit of Krusell and Smith (1998), a one-asset New Keynesian model in the spirit of McKay, Nakamura, and Steinsson (2016), and a two-asset New Keynesian model in the spirit of Kaplan, Moll, and Violante (2018). Table I illustrates the speeds that our algorithms are able to achieve on a laptop computer.[2] For each of our three models (including a high-dimensional version of the Krusell–Smith model), it takes less than 11 seconds to compute the heterogeneous-agent Jacobians $\mathcal{J}$. Once these Jacobians are known, it is almost immediate to calculate impulse responses. Posterior-mode estimation takes less than 9

[2]All computations were performed on a laptop with a 2.6 GHz Intel Core i7-10750H processor with six cores.

TABLE I

SUMMARY OF COMPUTING TIMES[a]

Computing Times	Req.	Krusell–Smith	HD Krusell–Smith	One-Asset HANK	Two-Asset HANK
Steady state (s.s.)		0.42 s	52.08 s	1.88 s	16.16 s
Heterogeneous-agent Jacobians ($\mathcal{J}$)	s.s.	0.09 s	10.47 s	0.32 s	3.50 s
One impulse response	$\mathcal{J}$	0.0009 s	0.0009 s	0.0136 s	0.0263 s
All impulse responses (**G**)	$\mathcal{J}$	0.0033 s	0.0033 s	0.0506 s	0.1735 s
Simulation (100,000 periods)	**G**	0.0040 s	0.0050 s	0.0219 s	0.1047 s
Bayesian estimation (shocks)	**G**				
single likelihood evaluation		0.0007 s	0.0007 s	0.0024 s	0.0140 s
obtaining posterior mode		0.06 s	0.06 s	0.66 s	16.22 s
RWMH (200,000 draws)		132 s	132 s	568 s	2900 s
Bayesian estimation (shocks + model)	$\mathcal{J}$				
single likelihood evaluation		—	—	0.056 s	0.227 s
obtaining posterior mode		—	—	14 s	522 s
RWMH (200,000 draws)		—	—	11,218 s	42,564 s
Nonlinear impulse responses	$\mathcal{J}$	0.32 s	27.85 s	1.17 s	14.63 s
No. of idiosyncratic states		3500	250,000	3500	10,500
Time horizon (T)		300	300	300	300
No. of shock parameters in estimation		3	3	6	14
No. of model parameters in estimation		0	0	3	5

[a]The times given are incremental, with the "Req." column denoting the prerequisite step for each computation. RWMH refers to Random Walk Metropolis–Hastings. Our Krusell–Smith model and its "high-dimensional" (HD) version are described in Section 2. Our one-asset HANK model is described in Appendix B.2. Our two-asset HANK model is described in Appendix B.3. All calculations in this paper were performed on a laptop with a 2.6 GHz Intel Core i7-10750H processor with six cores.

minutes for every model, and is, for simpler models, a matter of seconds or milliseconds. A standard Random Walk Metropolis–Hastings algorithm that traces out the posterior distribution of parameters with 200,000 draws takes less than twelve hours for our most complex, two-asset HANK model. By contrast, the leading computational techniques existing today find it challenging to estimate a two-asset HANK model at all.

Related Literature. Since the early breakthroughs of Krusell and Smith (1998) and den Haan (1997), the literature on solution methods for heterogeneous-agent models has grown tremendously. Part of the literature has developed nonlinear methods, which are well-suited to address questions that inherently involve higher-order aggregate moments, such as the aggregate implications of risk premia or volatility shocks.[3] However, when it comes to the distribution of agents, these methods typically require either limited heterogeneity, or "approximate aggregation" (where only a few moments of the distribution matter for forecasting general equilibrium dynamics).

Our paper, by contrast, follows Reiter (2009) by linearizing with respect to aggregates but preserving nonlinearities with respect to idiosyncratic shocks. The Reiter method can be used to solve models that do not feature approximate aggregation, and instead capture the rich interactions between the distribution of agents and macroeconomic outcomes that are the hallmark of the recent heterogeneous-agent literature (see, e.g., Krueger, Mitman, and Perri (2016) and Kaplan and Violante (2018)). Its main limitation

[3]See the survey by Algan, Allais, Den Haan, and Rendahl (2014) and recent work by Brumm and Scheidegger (2017), Mertens and Judd (2018), Proehl (2019), and Fernández-Villaverde, Hurtado, and Nuño (2019), among many others.

is that it involves a linear system that grows with the dimension of the state space of the heterogeneous-agent model. For many complex models, the Schur (or equivalent) decomposition required to solve these models becomes too costly. This has led the literature to turn to "model reduction" methods, which involve approximating the equilibrium distribution, and sometimes also the value function.[4] How accurately these methods match the solution without model reduction varies depending on the application.[5] Our method, by contrast, solves the unreduced model, leaving all heterogeneity intact.

Boppart, Krusell, and Mitman (2018) also proposed a sequence-space method that solves the unreduced model and avoids the need for a large state-space system. They solved nonlinearly for impulse responses to one-time, unanticipated aggregate shocks ("MIT shocks"); when the shocks are small, this gives approximately the model's linear impulse responses. This method, however, requires some way to solve for nonlinear impulse responses in the first place. Boppart, Krusell, and Mitman (2018) followed the typical approach by iterating over guesses for aggregate sequences, but there is no general method for updating these guesses, nor any guarantee of convergence.[6] By exploiting linearity instead, we avoid the need for any iteration, achieving the stability and speed required for advanced applications such as estimation.[7]

Layout. The rest of the paper proceeds as follows. Section 2 introduces our computational method with an example. Section 3 provides our fast algorithm for computing the Jacobians of heterogeneous-agent problems. Section 4 shows how to efficiently combine these Jacobians to compute general equilibrium impulse responses. Section 5 provides our application to estimation, and Section 6 our application to nonlinear transitions. Section 7 concludes.

2. THE SEQUENCE-SPACE JACOBIAN: AN EXAMPLE

We introduce our methods by means of an example: Krusell and Smith (1998)'s celebrated extension of the real business cycle model to heterogeneous households. This model is a natural starting point, since it is well known and there exist many well-established methods for solving it.

We set up the model in the sequence space, that is, assuming perfect foresight with respect to aggregates. We then show how to use the sequence-space Jacobian to solve for the impulse response of the model to a total factor productivity (TFP) shock in a fraction of a second.

[4]See, for instance, Reiter (2010), Ahn, Kaplan, Moll, Winberry, and Wolf (2018), Winberry (2018), and Bayer and Luetticke (2020).

[5]For instance, Ahn et al. (2018) showed that their model reduction technique works well for a one-asset model, but that it is more difficult to achieve a good fit for a two-asset model; they were able to reduce the size of the state-space system for the latter to 2445-by-2445, but further reduction degrades accuracy.

[6]In Section 6, we propose such a method for updating guesses using sequence-space Jacobians. It would be redundant, however, to use this method to obtain linear impulse responses, since we can solve directly for these responses from the Jacobians.

[7]We share with all aggregate linearization methods the drawback that the model does not generate risk premia, portfolio choice is indeterminate, and optimal Ramsey policy is ill-defined. For these applications, higher-order perturbations or global solution methods are more appropriate (see, e.g., Fernández-Villaverde, Rubio-Ramírez, and Schorfheide (2016)).

2.1. *Model Description*

The economy is populated by a mass 1 of heterogeneous households that maximize the time-separable utility function $\mathbb{E}[\sum \beta^t u(c_t)]$, where u has the standard constant relative risk aversion form, $u(c) = \frac{c^{1-\sigma}}{1-\sigma}$. There exist n_e idiosyncratic states, and in any period t, agents transition between any two such states e and e' with exogenous probability $P(e, e')$. We denote by π the stationary distribution of P and assume that the mass of agents in each state e is always equal to $\pi(e)$.[8] Agents supply an exogenous number of hours n, and earn wage income $w_t e n$, where w_t is the wage per efficient hour. Agents can only trade in capital k, which pays a rental rate r_t net of depreciation, and are subject to a no-borrowing constraint. The value function of an agent entering the period in income state e and with capital k_- at time t is therefore

$$\begin{aligned} V_t(e, k_-) = \max_{c,k} u(c) + \beta \sum_{e'} V_{t+1}(e', k) P(e, e') \\ \text{s.t.} \quad c + k = (1 + r_t)k_- + w_t e n, \\ k \geq 0. \end{aligned} \tag{2}$$

Denote by $c_t^*(e, k_-)$ and $k_t^*(e, k_-)$ the policy functions that solve the Bellman equation (2). Also denote by $D_t(e, K_-) \equiv \Pr(e_t = e, k_{t-1} \in K_-)$ the measure of households in state e that own capital in a set K_- at the start of date t. The distribution D_t has law of motion

$$D_{t+1}(e', K) = \sum_e D_t(e, k_t^{*-1}(e, K)) P(e, e'), \tag{3}$$

where $k_t^{*-1}(e, \cdot)$ denotes the inverse of $k_t^*(e, \cdot)$. We assume that prior to $t = 0$, the economy is in a steady state with constant wage w_{ss} and net rental rate r_{ss}, corresponding to a steady state of the general equilibrium economy discussed momentarily. In this steady state, there is a unique value function and decision rule solving (2), and a unique stationary distribution D_{ss} solving (3). We suppose that agents start in this stationary distribution at date 0, so that $D_0 = D_{ss}$.

Equation (2) shows that, for any t, the policy $k_t^*(e, k_-)$ is a function of the future path $\{r_s, w_s\}_{s \geq t}$. Given $D_0 = D_{ss}$, through (3), the distribution $D_t(e, K)$ at any t is a function of the entire path $\{r_s, w_s\}_{s \geq 0}$.[9] It follows that aggregate household capital holdings are characterized by a *capital function* $\mathcal{K}_t(\{r_s, w_s\}_{s \geq 0})$, where

$$\mathcal{K}_t(\{r_s, w_s\}_{s \geq 0}) = \sum_e \int_{k_-} k_t^*(e, k_-) D_t(e, dk_-). \tag{4}$$

The ability to reduce interactions between heterogeneous agents to functions such as $\mathcal{K}_t$, which map aggregate sequences into aggregate sequences, is key to the sequence-space

[8] In the original Krusell and Smith (1998) model, the transition probabilities depend on the aggregate state, that is, P takes the form $P(e, e', Z_t)$. Our methods can be applied to this case as well (see the general formulation in Appendix A of the Supplemental Material (Auclert, Bardóczy, Rognlie, and Straub (2021))).

[9] This can be shown recursively: given $D_0 = D_{ss}$, D_1 is a function of $\{r_s, w_s\}_{s \geq 0}$, and therefore so is D_2, through its dependence on D_1. In Section 3, we elicit explicitly the first-order dependence of D_t, k_t^*, and $\mathcal{K}_t$ on the sequence $\{r_s, w_s\}_{s \geq 0}$.

Jacobian method. We now combine this $\mathcal{K}_t$ function with equations describing production and market-clearing conditions to describe the entire Krusell–Smith economy. Production is carried out by a competitive representative firm, which has a Cobb–Douglas technology $Y_t = Z_t K_{t-1}^{\alpha} N_t^{1-\alpha}$, rents capital and labor from workers at rates $r_t + \delta$ and w_t, and faces the sequence of total factor productivity Z_t. The firm's first-order conditions

$$r_t = \alpha Z_t \left(\frac{K_{t-1}}{N_t}\right)^{\alpha-1} - \delta, \tag{5}$$

$$w_t = (1-\alpha) Z_t \left(\frac{K_{t-1}}{N_t}\right)^{\alpha} \tag{6}$$

relate the paths of prices $\{r_t, w_t\}$ to the exogenous paths $\{Z_t, N_t = \sum \pi(e) e n\}$ and the endogenous path for capital $\{K_t\}$. Combining (4)–(6), we can express the capital market-clearing condition at each point in time as a function H,

$$H_t(\mathbf{K}, \mathbf{Z}) \equiv \mathcal{K}_t\left(\left\{\alpha Z_s \left(\frac{K_{s-1}}{\sum \pi(e) e n}\right)^{\alpha-1} - \delta, (1-\alpha) Z_s \left(\frac{K_{s-1}}{\sum \pi(e) e n}\right)^{\alpha}\right\}_{s\geq 0}\right) - K_t = 0, \tag{7}$$

where $\mathbf{K} = (K_0, K_1, \ldots)'$. Given initial capital K_{-1} and the exogenous path for productivity, $\mathbf{Z} = (Z_0, Z_1, \ldots)'$, equation (7) pins down the equilibrium path of capital.

2.2. *Impulse Responses*

Applying the implicit function theorem to (7), the linear impulse response of capital to a transitory technology shock $d\mathbf{Z} = (dZ_0, dZ_1, \ldots)'$ is given by

$$d\mathbf{K} = -\mathbf{H}_{\mathbf{K}}^{-1} \mathbf{H}_{\mathbf{Z}}\, d\mathbf{Z}, \tag{8}$$

where $\mathbf{H}_{\mathbf{K}}$ and $\mathbf{H}_{\mathbf{Z}}$ denote the Jacobians of $\mathbf{H}$ with respect to $\mathbf{K}$ and $\mathbf{Z}$, evaluated at the steady state. Given $d\mathbf{K}$, the impulse responses of other variables, for example, $\{Y_s, r_s, w_s\}$, follow immediately. In practice, (8) is solved up to a given (large) horizon T such that K and Z have approximately returned to steady state by time T.

We use the chain rule to relate the Jacobians $\mathbf{H}_{\mathbf{K}}$ and $\mathbf{H}_{\mathbf{Z}}$ to the derivatives of the $\mathcal{K}$ function defined in equation (4), evaluated at the steady state. For example, differentiating equation (7) with respect to K_s, we find that the t, s entry of $\mathbf{H}_{\mathbf{K}}$ is

$$[\mathbf{H}_{\mathbf{K}}]_{t,s} = \frac{\partial \mathcal{K}_t}{\partial r_{s+1}} \frac{\partial r_{s+1}}{\partial K_s} + \frac{\partial \mathcal{K}_t}{\partial w_{s+1}} \frac{\partial w_{s+1}}{\partial K_s} - 1_{\{s=t\}}. \tag{9}$$

A similar expression applies to $\mathbf{H}_{\mathbf{Z}}$. In addition, the derivatives $\frac{\partial r_{s+1}}{\partial K_s}$, $\frac{\partial w_{s+1}}{\partial K_s}$, $\frac{\partial r_{s+1}}{\partial Z_s}$, and $\frac{\partial w_{s+1}}{\partial Z_s}$ at $(\mathbf{K}_{ss}, \mathbf{Z}_{ss})$ can all be computed analytically: for example,

$$\frac{\partial r_{s+1}}{\partial K_s} = \alpha(\alpha-1) Z_{ss} \left(\frac{K_{ss}}{N_{ss}}\right)^{\alpha-2} \frac{1}{N_{ss}}.$$

Hence, to obtain $\mathbf{H}_{\mathbf{K}}^{-1} \mathbf{H}_{\mathbf{Z}}$ in (8), all we need are the Jacobians of the $\mathcal{K}$ function with respect to its two inputs r and w. The key remaining challenge is to compute these Jacobians. In the next section, we introduce a fast algorithm for doing so. As Table I reveals, for a standard calibration of the Krusell–Smith model detailed in Appendix B.1,

(a) AR(1) shock with persistence ρ (b) News shock at time s

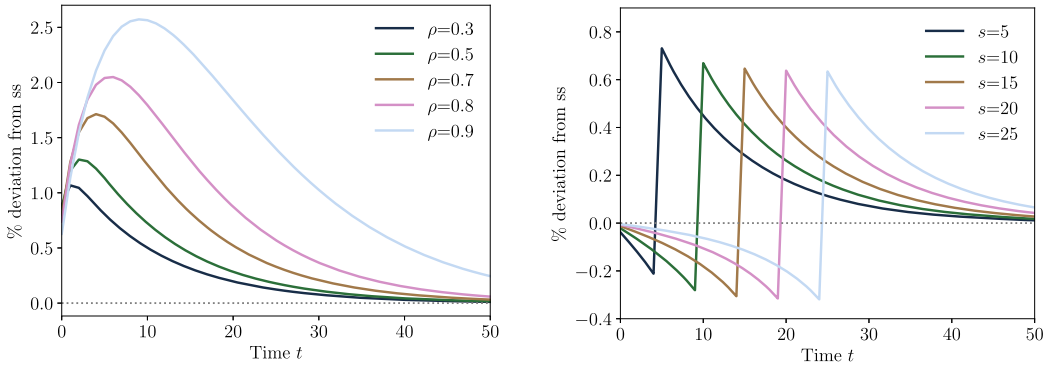

FIGURE 1.—Impulse responses of capital to 1% TFP shocks in the Krusell–Smith model.

this algorithm takes 90 milliseconds to calculate Jacobians of $\mathcal{K}$, truncated to a horizon of 300×300.[10] In a "high-dimensional" calibration that increases the dimensionality of the state space from 3500 to 250,000, it still takes less than 11 seconds.

Given these Jacobians, the underlying heterogeneity no longer matters: the Jacobians tell us everything that we need to know, to first order, about the aggregate behavior of the model's heterogeneous agents. This feature of our method is apparent in Table I, where we see that most other computing times are identical between our two calibrations of the Krusell–Smith model, despite the large disparity in the size of their underlying state spaces.

Impulse Responses and News-Shock Interpretation. Once we have the Jacobians of $\mathcal{K}$, we can immediately calculate $-\mathbf{H}_{\mathbf{K}}^{-1}\mathbf{H}_{\mathbf{Z}}$. Given (8), applying this matrix to any path for $d\mathbf{Z}$ delivers the impulse response $d\mathbf{K}$ of capital with a single matrix-vector multiplication. Panel (a) of Figure 1 does this for a variety of $d\mathbf{Z}$, representing 1% AR(1) shocks to TFP with different persistences ρ in our high-dimensional Krusell–Smith model. Note that the same matrix is applied to all these $d\mathbf{Z}$ vectors: once we have computed an impulse response, it is almost costless to compute others.

It is, in particular, immediate to obtain the effect of the "news" at date 0 that TFP will be higher by 1% at time s, as in panel (b) of Figure 1. By definition, the impulse responses to s-period-ahead news are equal to the sth column of the matrix $-\mathbf{H}_{\mathbf{K}}^{-1}\mathbf{H}_{\mathbf{Z}}$. This "news-shock" interpretation of the columns provides a useful way of understanding their role in the computation of generic impulse responses. For example, the impulse responses to AR(1) TFP paths of persistence ρ in panel (a) can be reinterpreted as the effect of the simultaneous news, at date 0, of an increase of ρ^s in TFP at times $s = 0, 1, \ldots$.

3. COMPUTING JACOBIANS FOR HETEROGENEOUS-AGENT PROBLEMS

In the previous section, we established the usefulness of knowing the Jacobians $\partial\mathcal{K}/\partial r$ and $\partial\mathcal{K}/\partial w$ for computing the impulse responses of the Krusell–Smith model. In this section, we generalize the $\mathcal{K}$ function, to encompass the mapping from inputs to outputs

[10] This is long enough to accurately compute the solution given the shocks considered in Figure 1. We discuss how to choose an appropriate truncation horizon in Section 4.2.

in a broad class of heterogeneous-agent problems. In this general case, *inputs* are the aggregates relevant to the decision-making of individual agents, such as interest rates or wages, while *outputs* can describe aggregate savings, consumption, investment, or other decisions by heterogeneous households or firms. We introduce a fast algorithm, which we call the *fake news algorithm*, for computing the Jacobian of any output with respect to any input.

3.1. *General Model Representation*

We begin by introducing a generic representation of a heterogeneous-agent problem as a mapping between a time path of aggregate inputs $\mathbf{X}_t$ and a time path of aggregate outputs $\mathbf{Y}_t$. Assume that there are n_x inputs and n_y outputs, and that the distribution is discretized on n_g grid points. Let $\mathbf{D}_t$ be the $n_g \times 1$ vector representing the distribution of agents at time t, and suppose that the aggregate outputs of interest are the averages of individual "outcomes" against the distribution, that is, $\mathbf{Y}_t = \mathbf{y}_t' \mathbf{D}_t$, with $\mathbf{y}_t$ denoting the $n_g \times n_y$ matrix of individual outcomes (an outcome can be an agent's policy, e.g., consumption, or any other variable of interest defined at the individual level).[11] We assume that there exist three functions v, Λ, and y such that, for a given initial distribution $\mathbf{D}_0$, $\mathbf{Y}_t$ is the solution to the system of equations:

$$\mathbf{v}_t = v(\mathbf{v}_{t+1}, \mathbf{X}_t), \tag{10}$$

$$\mathbf{D}_{t+1} = \Lambda(\mathbf{v}_{t+1}, \mathbf{X}_t)' \mathbf{D}_t, \tag{11}$$

$$\mathbf{Y}_t = y(\mathbf{v}_{t+1}, \mathbf{X}_t)' \mathbf{D}_t. \tag{12}$$

Here, $\mathbf{X}_t$ is the $n_x \times 1$ vector of aggregate inputs. Equation (10) expresses how the vector representing the value function, $\mathbf{v}_t$, relates to $\mathbf{X}_t$ and to its own value in the next period. Equation (11) updates the distribution, with $\Lambda(\mathbf{v}_{t+1}, \mathbf{X}_t)$ an $n_g \times n_g$ transition matrix representing the discretized law of motion for this distribution. Finally, equation (12) defines the $n_y \times 1$ vector of aggregate outputs $\mathbf{Y}_t$, with the $n_g \times n_y$ matrix of individual outcomes $\mathbf{y}_t$ defined by $y(\mathbf{v}_{t+1}, \mathbf{X}_t)$. Later, we will argue that many heterogeneous-agent models indeed take this form.

For given $\mathbf{X}_{ss}$, the *steady state* of the model is the fixed point $(\mathbf{Y}_{ss}, \mathbf{v}_{ss}, \mathbf{D}_{ss})$ of (10)–(12) that obtains when $\mathbf{X}_t = \mathbf{X}_{ss}$ at all times. For convenience, we write $\Lambda_{ss} \equiv \Lambda(\mathbf{v}_{ss}, \mathbf{X}_{ss})$ and $\mathbf{y}_{ss} \equiv y(\mathbf{v}_{ss}, \mathbf{X}_{ss})$. We consider transitions of length T that end at this steady state, so that the terminal values are $\mathbf{X}_{T-1} = \mathbf{X}_{ss}$, and $\mathbf{v}_T = \mathbf{v}_{ss}$. The initial distribution $\mathbf{D}_0$ is given, and our main result assumes that it is also equal to $\mathbf{D}_{ss}$. Hence, this setting allows us to study transitory shocks around a steady state.[12]

Given this setup, (10)–(12) define a mapping from the $T \times n_x$ stacked vector of inputs $\mathbf{X}$, to the $T \times n_y$ stacked vector of outputs $\mathbf{Y}$, and we write this as

$$\mathbf{Y} = h(\mathbf{X}). \tag{13}$$

We assume that the functions v, Λ, and y are differentiable around $(\mathbf{v}_{ss}, \mathbf{X}_{ss})$, so that the function h is also differentiable around $\mathbf{X}_{ss}$. Our goal is to characterize the Jacobian $\mathcal{J}$

[11] As we show in Appendix A, it is straightforward to extend our method to include higher-order moments, such as the variance of consumption, among the outputs of interest.

[12] Section 6 discusses how to solve for nonlinear transition dynamics with arbitrary initial distributions $\mathbf{D}_0$, including the effects of permanent shocks that change the steady state.

of h evaluated at $\mathbf{X} = \mathbf{X}_{ss}$. $\mathcal{J}$ represents the aggregate response of heterogeneous agents to perturbations to their environment at different dates. This Jacobian can be of interest in its own right. But, critically, it is the key object required to compute the general equilibrium solution.

Example: Krusell and Smith. In the model of Section 2, the inputs are $\mathbf{X}_t = (r_t, w_t)$, and one natural choice for outputs is $\mathbf{Y}_t = (K_t, C_t)$. The model can be solved with value function iteration. In this case, $\mathbf{v}_t$ is the value function V_t in equation (2) at each point on the grid for states (e, k_-), and $\mathbf{D}_t$ is the fraction of agents at time t at each point on this grid. Given $\mathbf{v}_{t+1}$ and $\mathbf{X}_t$, the solution to (2) involves a maximized value function $\mathbf{v}_t$—equation (10)—and a policy function $\mathbf{k}_t$. We use the Young (2010) lottery method to convert this policy into a transition matrix on the grid, and compose this with the process for e to obtain the full transition matrix Λ_t' from current states (e, k_-) to next-period states (e', k)—equation (11). Finally, aggregate capital and consumption are obtained by taking the dot product of the policies $\mathbf{k}_t$ and $\mathbf{c}_t$ with the distribution $\mathbf{D}_t$: this is equation (12), with $\mathbf{y}_t \equiv (\mathbf{k}_t, \mathbf{c}_t)$.

An alternative approach, which is typically faster and more accurate in practice, is to use the Euler equation, as in Carroll (2006). In this approach, $\mathbf{v}_t$ is the derivative of the value function $\frac{\partial V_t}{\partial k_-}$ at each point on the grid for (e, k_-). The Euler equation maps $\mathbf{v}_{t+1}$ and $\mathbf{X}_t$ to optimal capital and consumption policies $\mathbf{k}_t$ and $\mathbf{c}_t$, and the envelope theorem implies $\mathbf{v}_t = (1 + r_t)u'(\mathbf{c}_t)$. Combining these, we obtain equation (10). Again, combining $\mathbf{k}_t$ with the exogenous law of motion for the state e delivers Λ in equation (11), and $\mathbf{y}_t \equiv (\mathbf{k}_t, \mathbf{c}_t)$ aggregates individual policies into K_t and C_t in equation (12).

Beyond this example, many other heterogeneous-agent problems can also be cast into the framework of equations (10)–(12). The scope and limitations of our framework will become clearer after we have presented our algorithm, so we postpone this discussion to the end of the next section.

3.2. *Fake News Algorithm*

In this section, we provide a fast algorithm for computing $\mathcal{J}$, which we call the "fake news" algorithm. We start with two preliminaries: notational conventions, and a direct method for computing $\mathcal{J}$ that will serve as a benchmark for our algorithm.

Notation. To present our algorithm in an intuitive manner, we start by assuming that there is only one input and one output, $n_x = n_y = 1$, and later generalize to any n_x and n_y. Define the $T \times 1$ vector $\mathbf{e}^s$ to have 0's everywhere except at the sth entry, where it has a 1. For a given dx, we say there is a "shock at time s" when the $T \times 1$ input vector is given by $\mathbf{X}^s \equiv \mathbf{X}_{ss} + \mathbf{e}^s\, dx$. Let $\mathbf{v}_t^s$, $\mathbf{D}_t^s$, and Y_t^s denote the solution to equations (10)–(12) given $\mathbf{X}^s$. Also, let $\Lambda_t^s \equiv \Lambda(\mathbf{v}_{t+1}^s, X_t^s)$ denote the transition matrix between states at time t, and $\mathbf{y}_t^s \equiv y(\mathbf{v}_{t+1}^s, X_t^s)$ denote the outcome function at time t, in response to the shock at time s. Finally, denote with a d the difference of all objects relative to their steady-state level, so that $dY_t^s \equiv Y_t^s - Y_{ss}$, $d\mathbf{y}_t^s \equiv \mathbf{y}_t^s - \mathbf{y}_{ss}$, $d\Lambda_t^s \equiv \Lambda_t^s - \Lambda_{ss}$, and $d\mathbf{D}_t^s \equiv \mathbf{D}_t^s - \mathbf{D}_{ss}$. The sth column of the Jacobian $\mathcal{J}$ is then the limit of $\frac{d\mathbf{Y}^s}{dx}$ as $dx \to 0$.

Direct Method. A direct method for computing the sth column of the Jacobian using one-sided numerical differentiation is as follows. First, starting with a small shock dx at time s, iterate (10) backward, starting with $\mathbf{v}_T = \mathbf{v}_{ss}$, and compute the value function $\mathbf{v}_t^s$, the transition matrix Λ_t^s, and individual policies $\mathbf{y}_t^s$, for $t = T - 1, \ldots, 0$. Second,

iterate (11) forward, starting with $\mathbf{D}_0 = \mathbf{D}_{ss}$, to solve recursively for the distributions $\mathbf{D}_t^s$ for $t = 1, \ldots, T-1$, by applying the transition matrices Λ_t^s. Next, for each t, take the distribution-weighted sum $(\mathbf{y}_t^s)'\mathbf{D}_t^s$ of individual policies to obtain Y_t^s in (12). Finally, form $\mathcal{J}_{t,s} = dY_t^s/dx = (Y_t^s - Y_{ss})/dx$. To obtain the entire Jacobian $\mathcal{J}$, repeat this process T times, once for each s. This is costly in practical applications, since T is typically at least equal to 300.

Structure of Jacobian $\mathcal{J}$. We now turn to our algorithm, which relies on several results about the structure of the Jacobian $\mathcal{J}$. The key is to recognize that the columns of $\mathcal{J}$ are closely related. Using our s superscript notation, equation (12) defines the output at time t in response to the shock at time s as

$$Y_t^s = \left(\mathbf{y}_t^s\right)'\mathbf{D}_t^s, \tag{14}$$

and (11) defines the distribution at time $t+1$ given the shock at time s as

$$\mathbf{D}_{t+1}^s = \left(\Lambda_t^s\right)'\mathbf{D}_t^s. \tag{15}$$

We first show how to efficiently obtain the policy functions $\mathbf{y}_t^s$ and transition matrices Λ_t^s. This makes use of the following implication of dynamic programming.

LEMMA 1: *For any $s \geq 1$, $t \geq 1$, we have*

$$\mathbf{y}_t^s = \begin{cases} \mathbf{y}_{ss}, & s < t, \\ \mathbf{y}_{T-1-(s-t)}^{T-1}, & s \geq t, \end{cases} \quad \textit{and} \quad \Lambda_t^s = \begin{cases} \Lambda_{ss}, & s < t, \\ \Lambda_{T-1-(s-t)}^{T-1}, & s \geq t. \end{cases} \tag{16}$$

Lemma 1 follows immediately from the recursive structure of equation (10) and the definition of $\mathbf{y}_t^s$ and Λ_t^s. The intuition is that agents only care about the distance to the shock $s - t$, rather than calendar time t and s separately, when deciding on their own behavior. For instance, the response of their consumption policy at time t to any shock at time $t+1$ is the same as the response of their consumption policy at time 0 to the same shock at time 1.

By implication, we can compute *all* policies $\mathbf{y}_t^s$ from a single perturbation of the input at date $s = T-1$. The same argument applies to the transition matrices Λ_t^s. Lemma 1 therefore suggests an immediate improvement to the direct algorithm for computing the Jacobian: replace the T backward iterations by a single backward iteration starting from a shock at date $T-1$. This is enough to deliver all policy functions $\mathbf{y}_t^s$ and Λ_t^s for all shock dates s and all t. Observe that this result is true nonlinearly, that is, irrespective of the size of dx.

Our next result speeds up the algorithm even further, for the case in which the transition begins and ends at the same steady state ($\mathbf{D}_0 = \mathbf{D}_{ss}$) and the shock dx is infinitesimal. The result concerns aggregate outcomes Y_t^s. For any $s \geq 1$, $t \geq 1$, we define

$$\mathcal{F}_{t,s} \cdot dx \equiv dY_t^s - dY_{t-1}^{s-1} \tag{17}$$

as the difference between the aggregate response of the output at t to a shock at date s, and its response at $t-1$ to a shock at date $s-1$. Since equation (16) implies that $d\mathbf{y}_t^s = d\mathbf{y}_{t-1}^{s-1}$ for all $s, t \geq 1$, one might conjecture that $\mathcal{F}_{t,s}$ is identically zero. But this conjecture is not quite right, since the distribution in equation (14) is also changing over time. The next lemma characterizes $\mathcal{F}_{t,s}$.

LEMMA 2: *Assume that* $\mathbf{D}_0 = \mathbf{D}_{ss}$. *For infinitesimal* dx, *and any* $s \geq 1$, $t \geq 1$, *we have*

$$\mathcal{F}_{t,s} \cdot dx = \mathbf{y}'_{ss} \left(\Lambda'_{ss}\right)^{t-1} d\mathbf{D}_1^s. \tag{18}$$

PROOF: First, since $\mathbf{D}_0 = \mathbf{D}_{ss}$, in the absence of any shock ($dx = 0$) we have $Y_t = Y_{ss}$, $\mathbf{y}_t^s = \mathbf{y}_{ss}$, and $\mathbf{D}_t^s = \mathbf{D}_{ss}$ for all t. Since y and Λ are differentiable, in the limit as $dx \to 0$, equation (14) implies

$$dY_t^s = \mathbf{y}'_{ss}\, d\mathbf{D}_t^s + \left(d\mathbf{y}_t^s\right)' \mathbf{D}_{ss}. \tag{19}$$

Subtracting dY_t^s and dY_{t-1}^{s-1} and using the fact that equation (16) implies $d\mathbf{y}_t^s = d\mathbf{y}_{t-1}^{s-1}$, we obtain

$$\mathcal{F}_{t,s} \cdot dx = \mathbf{y}'_{ss} \left(d\mathbf{D}_t^s - d\mathbf{D}_{t-1}^{s-1}\right). \tag{20}$$

Next, in the limit as $dx \to 0$, equation (15) implies both

$$d\mathbf{D}_t^s = \Lambda'_{ss}\, d\mathbf{D}_{t-1}^s + \left(d\Lambda_{t-1}^s\right)' \mathbf{D}_{ss} \tag{21}$$

and

$$d\mathbf{D}_{t-1}^{s-1} = \Lambda'_{ss}\, d\mathbf{D}_{t-2}^{s-1} + \left(d\Lambda_{t-2}^{s-1}\right)' \mathbf{D}_{ss}.$$

Subtracting and using the fact that equation (16) implies $d\Lambda_{t-1}^s = d\Lambda_{t-2}^{s-1}$, we therefore finally have simply

$$\begin{aligned} d\mathbf{D}_t^s - d\mathbf{D}_{t-1}^{s-1} &= \Lambda'_{ss} \left(d\mathbf{D}_{t-1}^s - d\mathbf{D}_{t-2}^{s-1}\right) \\ &= \left(\Lambda'_{ss}\right)^2 \left(d\mathbf{D}_{t-2}^s - d\mathbf{D}_{t-3}^{s-1}\right) \\ &\;\;\vdots \\ &= \left(\Lambda'_{ss}\right)^{t-1} d\mathbf{D}_1^s, \end{aligned} \tag{22}$$

where the last line follows because, given that $\mathbf{D}_0 = \mathbf{D}_{ss}$, we have $d\mathbf{D}_0^{s-1} = 0$ for all $s \geq 1$. *Q.E.D.*

The intuition for equation (18) is as follows. Suppose that we know the path of the aggregate output Y_t at all dates $t = 0, \ldots, T-1$ in response to a shock at date $s-1$. How does this compare to the path of Y_t in response to a shock at date s, from date $t = 1$ onwards? From Lemma 1, the behavior of agents at all dates is identical in both cases. Therefore, the only difference is that the initial distribution in the second case is $\mathbf{D}_1^s$ rather than $\mathbf{D}_{ss}$. To first order, this difference in initial distribution affects aggregates at all dates as if agents followed their steady-state behavior, which is what equation (18) expresses.

For a given s, $\mathcal{F}_{t,s}$ can be interpreted as the impulse response to a "date-s fake news shock": a shock to date s announced at date 0, and retracted at date 1.[13] At date 0, agents react to the announcement, which leads to the distribution $\mathbf{D}_1^s$. After the announcement

[13]This information structure is the same as that used by Christiano et al. (2010) to generate a boom-bust episode in response a shock to productivity that later turns out not to happen. In our case, the "fake news" shock for date s is unlearned at date 1. It is also related, though not formally equivalent, to the "noise shocks" considered in the belief-driven business cycle literature literature (e.g., Lorenzoni (2009)).

is retracted, they revert to steady-state policies, so the effect on output at all dates $t \geq 1$ is $\mathbf{y}'_{ss} \cdot (\Lambda'_{ss})^{t-1} d\mathbf{D}_1^s$. This expression can usefully be rewritten with the help of the following definition.

DEFINITION 1: The *expectation vector* for outcome y at time t is defined by

$$\mathcal{E}_t \equiv (\Lambda_{ss})^t \mathbf{y}_{ss}. \tag{23}$$

For each grid point, the time path of $\mathcal{E}_t$ represents the expected time path of outcome y, in the steady state, for an agent starting at that grid point.[14] Equation (18) then reads $\mathcal{F}_{t,s} \cdot dx = \mathcal{E}'_{t-1} d\mathbf{D}_1^s$.

We can now use Lemmas 1 and 2 to arrive at the following proposition.

PROPOSITION 1: *Assume that* $\mathbf{D}_0 = \mathbf{D}_{ss}$. *For infinitesimal* dx, *define the* (t, s)*th element of the* fake news matrix $\mathcal{F}$ *as*

$$\mathcal{F}_{t,s} \cdot dx \equiv \begin{cases} dY_0^s, & t = 0, \\ \mathcal{E}'_{t-1} d\mathbf{D}_1^s, & t \geq 1, \end{cases} \tag{24}$$

where $dY_0^s = (d\mathbf{y}_0^s)' \mathbf{D}_{ss}$ *and* $d\mathbf{D}_1^s = (d\Lambda_0^s)' \mathbf{D}_{ss}$. *Then, the Jacobian* $\mathcal{J}$ *of* h *satisfies the recursion* $\mathcal{J}_{t,s} = \mathcal{J}_{t-1,s-1} + \mathcal{F}_{t,s}$ *for* $t, s \geq 1$, *with* $\mathcal{J}_{t,s} = \mathcal{F}_{t,s}$ *for* $t = 0$ *or* $s = 0$, *and is therefore given by*

$$\mathcal{J}_{t,s} = \sum_{k=0}^{\min\{s,t\}} \mathcal{F}_{t-k,s-k}. \tag{25}$$

PROOF: When $t, s \geq 1$, the recursion immediately follows from Lemma 1. When $t = 0$, $\mathcal{J}_{t,s} \cdot dx = \mathcal{F}_{t,s} \cdot dx = dY_0^s$ by definition.

Finally, when $s = 0$ and $t \geq 1$, Lemma 1 implies that $d\mathbf{y}_t^0 = 0$, and by equation (19), we have $\mathcal{J}_{t,0} \cdot dx = dY_t^0 = \mathbf{y}'_{ss} d\mathbf{D}_t^0$. Since $d\Lambda_t^0 = 0$ for all $t \geq 1$, using (21) we can write $\mathcal{J}_{t,0} \cdot dx = \mathbf{y}'_{ss} d\mathbf{D}_t^0 = \mathbf{y}'_{ss} \Lambda'_{ss} d\mathbf{D}_{t-1}^0 = \cdots = \mathbf{y}'_{ss} (\Lambda'_{ss})^{t-1} d\mathbf{D}_1^0 = \mathcal{E}'_{t-1} d\mathbf{D}_1^0$, which is $\mathcal{F}_{t,0} \cdot dx$ in (24). *Q.E.D.*

Proposition 1 characterizes the first-order aggregate response of heterogeneous agents to changes in their environment at any date s, as a function of *only* dY_0^s (the aggregate initial response to shocks at date s), $d\mathbf{D}_1^s$ (the response of the distribution at date 1 to shocks at date s), and the expectation vectors $\mathcal{E}_t$ which can be obtained from the stationary solution. The intuition goes back to Lemmas 1 and 2: since policy functions only depend on the distance to the shock, and since the steady-state expectation vectors $\mathcal{E}_t$ give information about the behavior of aggregates after shocks to the initial distribution, it is possible to project the effect at any date t from knowledge of the effects of future shocks on aggregates and distributions at date 0. The expectation vectors, in turn, are easy to compute thanks to the following observation.

LEMMA 3: *The expectation vectors defined in* (23) *solve the recursion* $\mathcal{E}_t = \Lambda_{ss} \mathcal{E}_{t-1}$, *with* $\mathcal{E}_0 = \mathbf{y}_{ss}$.

[14] In the literature on control theory, the matrix with rows $\mathcal{E}'_0, \mathcal{E}'_1, \ldots$ is sometimes called the *observability matrix*. This concept was also used by Reiter (2010) and Ahn et al. (2018).

Algorithm for a Single Input and Output. Proposition 1 and Lemma 3 inspire our fast "fake news" algorithm. When implemented with one-sided numerical differentiation, given a small $dx > 0$, the algorithm consists of four steps:

1. Calculate $\mathbf{y}_0^s$ and Λ_0^s for each s using a single backward iteration from time $T-1$. Combining these with the initial steady-state distribution, form two key objects: the T scalars $\mathcal{Y}_s$ defined by $\mathcal{Y}_s\,dx \equiv dY_0^s = (d\mathbf{y}_0^s)'\mathbf{D}_{ss}$, representing the effect on the output at date 0 from the shock to the input at date s; and the T $n_g \times 1$-vectors $\mathcal{D}_s\,dx \equiv d\mathbf{D}_1^s = (d\Lambda_0^s)'\mathbf{D}_{ss}$, giving the change in the distribution at date 1 from the shock at date s.[15]
2. Calculate the $T-1$ $n_g \times 1$ expectation vectors $\mathcal{E}_t \equiv (\Lambda_{ss})^t\mathbf{y}_{ss}$, using the recursion from Lemma 3.
3. Combine results from the previous two steps to form the fake news matrix $\mathcal{F}$ from Proposition 1. The first row ($t=0$) of this matrix contains the $\mathcal{Y}$'s from step 1, and other rows ($t \geq 1$) contain the product $\mathcal{E}_{t-1}'\mathcal{D}_s$ from steps 1 and 2:

$$\mathcal{F} = \begin{bmatrix} \mathcal{Y}_0 & \mathcal{Y}_1 & \mathcal{Y}_2 & \cdots & \mathcal{Y}_{T-1} \\ \mathcal{E}_0'\mathcal{D}_0 & \mathcal{E}_0'\mathcal{D}_1 & \mathcal{E}_0'\mathcal{D}_2 & & \mathcal{E}_0'\mathcal{D}_{T-1} \\ \mathcal{E}_1'\mathcal{D}_0 & \mathcal{E}_1'\mathcal{D}_1 & \mathcal{E}_1'\mathcal{D}_2 & & \mathcal{E}_1'\mathcal{D}_{T-1} \\ \vdots & \vdots & \vdots & & \vdots \\ \mathcal{E}_{T-2}'\mathcal{D}_0 & \mathcal{E}_{T-2}'\mathcal{D}_1 & \mathcal{E}_{T-2}'\mathcal{D}_2 & \cdots & \mathcal{E}_{T-2}'\mathcal{D}_{T-1} \end{bmatrix}. \tag{26}$$

4. Using Proposition 1, build up the Jacobian $\mathcal{J}_{t,s} = \mathcal{J}_{t-1,s-1} + \mathcal{F}_{t,s}$ recursively from its first row and first column. By equation (25), the element (t,s) of the Jacobian $\mathcal{J}$ is the sum of the (t,s) element of the $\mathcal{F}$ matrix and of all the elements on the diagonal to its immediate upper left in (26). For instance, we have $\mathcal{J}_{2,2} = \mathcal{E}_1'\mathcal{D}_2 + \mathcal{E}_0'\mathcal{D}_1 + \mathcal{Y}_0$.

At this stage, it is clear why this algorithm achieves significantly higher speed than the direct method for computing the Jacobian: it requires only the computation of the primitive objects $\mathcal{Y}_t$ and $\mathcal{D}_t$, which can be obtained with one backward iteration starting from a shock at $T-1$, and of $\mathcal{E}_t$, which can be obtained by recursive application of the steady-state transition matrix, starting with the vector $\mathbf{y}_{ss}$ of steady-state outcomes.

Example: Krusell and Smith. Panel (a) of Figure 2 displays several columns of the Jacobian $\mathcal{J}^{\mathcal{K},r}$ for the Krusell–Smith model of Section 2. By the news-shock interpretation, these columns represent the time path of aggregate capital accumulation $\{\mathcal{K}_t\}$ when households learn at date 0 about an increase in the rental rate r_s at various dates s.

When the shock takes place at date 0, households are surprised by a higher return on existing assets. They save some of this additional return (a standard wealth effect), accumulating assets that they later progressively decumulate. When the shock takes place at later dates $s > 0$, households also have an intertemporal substitution response, which leads them to save in anticipation of the increase in r. This generates a "tent" pattern in the Jacobian $\mathcal{J}$.

Proposition 1 shows that the columns of $\mathcal{J}$ reflect the accumulation of terms from the fake news matrix $\mathcal{F}$. The columns of that matrix are depicted in panels (b) and (c). The

[15] In practice, it is usually more accurate to compute the differences $d\mathbf{y}_0^s$ and $d\Lambda_0^s$ by subtracting "ghost runs" rather than steady states. That is, compute $\mathbf{y}_0^s$ as described for some small $dx > 0$. Repeat the same procedure with $dx = 0$ to get $\tilde{\mathbf{y}}_0^s$. Set $d\mathbf{y}_0^s = \mathbf{y}_0^s - \tilde{\mathbf{y}}_0^s$. This procedure is more accurate than subtracting steady-state values whenever those have not fully converged, that is, whenever $\tilde{\mathbf{y}}_0^s \neq \mathbf{y}_{ss}$. Do the same for $d\Lambda_0^s$. See Appendix C.1 of the Supplemental Material for more details on this and other ways to manage numerical error.

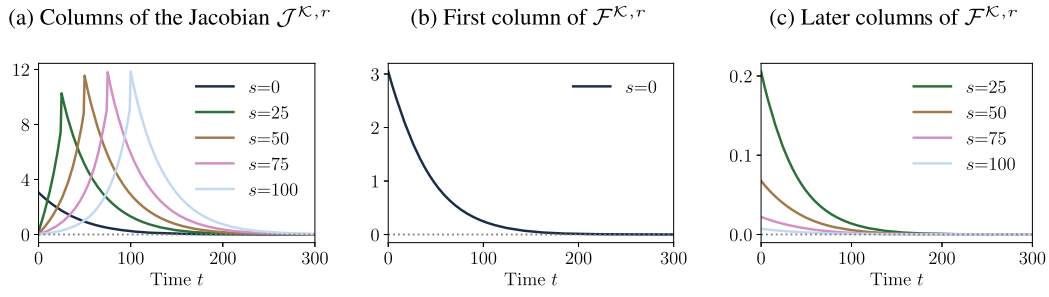

FIGURE 2.—Jacobian $\mathcal{J}^{\mathcal{K},r}$ and fake news matrix $\mathcal{F}^{\mathcal{K},r}$ in the Krusell–Smith model.

first column of $\mathcal{J}$ is the same as that of $\mathcal{F}$. By contrast, the other columns of $\mathcal{J}$ are a combination of a shifted-down version of the first column of $\mathcal{F}$ and of its other columns $\mathcal{F}_{\cdot s}$ for $s > 0$. By the "fake news" interpretation, these columns represent the behavior of aggregate assets when households first save at date 0 in anticipation of an increase in r at date s, and then dissave after the announcement is retracted at date 1.

One striking feature of the columns of the Jacobian $\mathcal{J}$ is that they converge to a regular pattern around the main diagonal: the $s = 50$ impulse response around $t = 50$ is almost the same as the $s = 75$ and $s = 100$ impulse responses around $t = 75$ and $t = 100$. In other words, if the shock is anticipated far enough in advance, all impulse responses are just shifted versions of each other. This reflects the fact that $\mathcal{F}_{t,s}$ goes to zero both for high t (the effect of date-0 behavior through the distribution dies away) and for high s (the effect of far-out shocks on date-0 behavior dies away), so that $\mathcal{J}_{t,s} \approx \mathcal{J}_{t-1,s-1}$ for high t and s.[16]

Generalization to Many Inputs and Outputs. In the general case in which the h function has multiple inputs i and outputs o, the algorithm above is straightforward to apply separately for each i and o. However, some further speed gain can be achieved by observing that certain objects can be reused several times. Specifically, the $\mathcal{D}_s$ depend only on the input shock dX^i, so they only need to be computed once per input and can be written as $\mathcal{D}^i_s$. Moreover, the $\mathcal{E}_t$ defined in step 2 depend only on the output of interest dY^o, so they only need to be computed once per output and can be written as $\mathcal{E}^o_t$. By contrast, the $\mathcal{Y}_s$ defined in step 1 depend on both the input shock dX^i and the output of interest dY^o. They are computed by doing a backward iteration in response to each input shock i, and then taking the aggregate response of each o for each s. This delivers a $\mathcal{Y}^{o,i}_s$ for each o and i. The $\mathcal{F}^{o,i}$ matrix can then be computed as in equation (26), but with $\mathcal{Y}^{o,i}$ in the first row, and the products $(\mathcal{E}^o_t)'\mathcal{D}^i_s$ in the other rows t, s.

Implementation and Accuracy. We suggested implementing our algorithm with one-sided numerical differentiation. This is simple in practice, but introduces small errors from the differentiation procedure. In Appendix C.1, we discuss alternatives, including two-sided numerical differentiation, which reduces error, and automatic differentiation, which eliminates it.

[16]This "asymptotic time invariance" property is a general feature of the Jacobians of heterogeneous-agent problems. A previous version of this paper (Auclert, Bardóczy, Rognlie, and Straub (2019)) provided a formal proof.

In Appendix D.1, we evaluate the errors when computing the Jacobian $\mathcal{J}^{\mathcal{K},r}$ in Figure 2. We use as a benchmark the Jacobian that results from the direct method with automatic differentiation.

The conclusions from this exercise are as follows. First, under automatic differentiation, the direct and the fake news method deliver exactly the same Jacobian, to near-machine precision. This verifies Proposition 1. Second, two-sided numerical differentiation is always more accurate than one-sided numerical differentiation, closing the gap with the automatic differentiation solution by one to two orders of magnitude. Third, when implemented with numerical differentiation, the fake news method is typically more accurate than the direct method. In all cases, the errors are small, less than 0.01% of the peak response.

Efficiency. Table II displays the time it takes to compute $\mathcal{J}$'s for the heterogeneous-agent block of each of our three benchmark models: the Krusell–Smith model already introduced, a one-asset HANK model with endogenous labor described in Appendix B.2, and a two-asset HANK model described in Appendix B.3. We report the times with one-sided numerical differentiation. The speed-up from using the fake news rather than the direct algorithm is very large in all cases: a factor of over 200 for all models.

What is the source of the large efficiency gain? When there are n_x inputs and n_y outputs, the direct algorithm discussed at the top of this section requires $n_x T^2$ backward "steps" and $n_x T^2$ forward "steps." By contrast, the fake news algorithm requires $n_x T$ backward steps and $n_y(T-1)$ applications of the matrix Λ_{ss} to construct the expectation vectors $\mathcal{E}_t$, reducing computational effort in steps 1 and 2 by a factor of around T, which in our application is $T = 300$.[17,18]

TABLE II

DIRECT AND FAKE NEWS ALGORITHMS TO COMPUTE 300×300 JACOBIANS $\mathcal{J}$

	Krusell–Smith	HD Krusell–Smith	One-Asset HANK	Two-Asset HANK
Direct	**21 s**	**2102 s**	**156 s**	**956 s**
step 1 (backward)	13 s	1302 s	132 s	846 s
step 2 (forward)	8 s	800 s	24 s	111 s
Fake news	**0.086 s**	**10.467 s**	**0.317 s**	**3.498 s**
step 1	0.060 s	8.654 s	0.236 s	3.159 s
step 2	0.011 s	1.061 s	0.022 s	0.119 s
step 3	0.011 s	0.758 s	0.045 s	0.201 s
step 4	0.003 s	0.003 s	0.014 s	0.018 s
Grid points n_g	3500	250,000	3500	10,500
Inputs n_x	2	2	4	5
Outputs n_y	2	2	4	4
Jacobians $n_x \times n_y$	4	4	16	20

[17]The computation of expectation vectors in step 2 takes far less time than the backward iteration in step 1, especially for the more complex models, because it only requires repeatedly multiplying by Λ_{ss}—which can be split into multiplication by a small transition matrix for the exogenous state, and multiplication by a highly sparse matrix with policies for endogenous states, both of which we implement efficiently.

[18]There are two additional steps required for the fast algorithm, steps 3 and 4. Step 3 involves the multiplication of $T \times n_g$ and $n_g \times T$ matrices, which has a cost proportional to $n_g T^2$ for each input-output pair—but since matrix multiplication is implemented extremely efficiently by standard numerical libraries, this is less of a

Jacobians as Sufficient Statistics for the Heterogeneous-Agent Problem. Since the Jacobians $\mathcal{J}$ locally describe the mapping $\mathbf{Y} = h(\mathbf{X})$, they are all that is needed to capture the local behavior of the heterogeneous-agent problem. This observation implies that all of the complexity introduced by heterogeneity in any given model boils down entirely to the Jacobian of the resulting heterogeneous-agent problem. This facilitates the analysis of the importance of heterogeneity for general equilibrium, and the connection of models to the data. For example, in simple general equilibrium models, the Jacobian of aggregate consumption with respect to income $\mathcal{J}^{C,y}$ is all that is needed for general equilibrium (Auclert, Rognlie, and Straub (2018)).

Scope and Limitations. In addition to the Krusell–Smith model, the two other models we consider in this paper fit into the framework of equations (10)–(12), so that the fake news algorithm applies to them directly. Our one-asset HANK model features a multidimensional choice over both labor and asset policies. Our two-asset HANK model features two endogenous states, a liquid and an illiquid asset.

A number of other models can also be directly cast into the framework of equations (10)–(12). This includes models where the inputs $\mathbf{X}$ matter directly for the transition rate between employment states (as in Gornemann, Kuester, and Nakajima (2016)), and models where higher-order moments of the distribution of agents are relevant as an output $\mathbf{Y}$ (such as the variance of consumption or a CES price index). It also includes models where some non-grid-based representation of the value function, such as Chebyshev polynomials, is used. Appendix A.1 covers these direct applications.

Other models require a slightly more general framework than (10)–(12). This includes models where the distribution of agents features entry and exit (e.g., Hopenhayn (1992) and simple overlapping generations models), or models where a nonlinear function of the distribution, such as the uth quantile function, is relevant. It also includes models where the distribution is represented parametrically, as in Algan, Allais, and Den Haan (2010). Appendix A.2 covers these more complex applications, which require a modification of Proposition 1, after which the fake news algorithm continues to apply.

Appendix A also covers how to approach models featuring discrete choice: for example, over the extensive margin of labor supply (e.g., Chang and Kim (2007)), or over resetting a price or investing in the presence of fixed costs (Golosov and Lucas (2007), Khan and Thomas (2008)). These fit into our original framework when taste shocks smooth out the discrete choice (Appendix A.1), and into our extended framework in other cases (Appendix A.2). Since these decision problems are often naturally posed in multiple stages, in Appendix A.3 we further extend our framework to accommodate multiple stages within each period.

Our extended framework in Appendix A allows for very general equations governing the distribution $\mathbf{D}_t$ and aggregate outputs $\mathbf{Y}_t$. An important limitation, however, is that it does not change the structure of equation (10); in particular, the value function $\mathbf{v}_t$ is not allowed to depend on $\mathbf{D}_t$. This prevents us from applying the fake news algorithm when the behavior of heterogeneous agents depends on the anticipated future distribution through the value function, in a way that cannot be intermediated via aggregates $\mathbf{X}_t$ in general equilibrium. This includes, for instance, OLG models with an endogenous distribution of bequests that are received in mid-life (e.g., de Nardi (2004), Straub (2017)), labor-search models with wage posting or individual bargaining (e.g., Burdett and Mortensen (1998),

bottleneck overall than the backward iteration in step 1, especially for models like the two-asset HANK where backward iteration is especially complex. Step 4 is even faster, since it is a simple recursion on $T \times T$ matrices.

Postel-Vinay and Robin (2002)), and money-search models where the anticipated distribution of cash balances matters directly for agent decisions (e.g., Molico (2006)).[19]

4. GENERAL EQUILIBRIUM IMPULSE RESPONSES

A typical general equilibrium heterogeneous-agent model consists of one or more heterogeneous-agent problems of the type described above, as well as additional sets of equations that govern production, market clearing, and so on. In this section, we explain how to solve for general equilibrium impulse responses once the Jacobians of the underlying heterogeneous-agent problem(s) are known.

4.1. *General Equilibrium in the Sequence Space*

A general equilibrium model in the sequence space is characterized by a system of nonlinear equations

$$\mathbf{F}(\mathbf{X}, \mathbf{Z}) = 0, \tag{27}$$

where $\mathbf{Z}$ denotes the path of exogenous "shocks," with $\mathbf{Z}_t$ an $n_z \times 1$ vector at each t, and $\mathbf{X}$ denotes the path of endogenous variables, with $\mathbf{X}_t$ an $n_x \times 1$ vector at each t. We assume that the model has as many equations as endogenous variables, and that it is *locally determinate*, that is, that $\mathbf{F}$ is invertible near the steady state $(\mathbf{X}^{ss}, \mathbf{Z}^{ss})$. Then, equation (27) truncated to a horizon of T is a nonlinear system of $n_x \times T$ equations in $n_x \times T$ endogenous variables, which delivers the general equilibrium impulse response to any change $d\mathbf{Z}$ in the path of $\mathbf{Z}$ relative to $\mathbf{Z}^{ss}$.

We solve for the impulse responses of the model to first order around the steady state. By the implicit function theorem, the response of endogenous variables $d\mathbf{X}$ to the shock $d\mathbf{Z}$ is given by

$$d\mathbf{X} = -\mathbf{F}_{\mathbf{X}}^{-1}\mathbf{F}_{\mathbf{Z}}\, d\mathbf{Z} \equiv \mathbf{G}\, d\mathbf{Z}, \tag{28}$$

where the Jacobians $\mathbf{F}_{\mathbf{X}}$ and $\mathbf{F}_{\mathbf{Z}}$ are evaluated at $(\mathbf{X}^{ss}, \mathbf{Z}^{ss})$, and we define $\mathbf{G}$ as the linear map from shocks $d\mathbf{Z}$ to general equilibrium impulse responses $d\mathbf{X}$.

Reducing Dimensionality With Variable Substitution. One difficulty with writing models in the form (27) is that the dimensionality can grow large enough that solving the linear system becomes a bottleneck. Quantitative DSGE models often have dozens of endogenous variables, which with $T = 500$ implies that $\mathbf{F}$ and $\mathbf{X}$ can have dimension 10,000 or higher.

In applications, it is common to reduce dimensionality by explicitly solving for some variables in terms of others. Suppose that $\mathbf{F}$ is separated into $\mathbf{F}_1$ and $\mathbf{F}_2$, and that $\mathbf{F}_2(\mathbf{X}, \mathbf{Z}) = 0$ can be solved in closed form to obtain $\mathbf{X}$ as a function of some smaller vector $\mathbf{U}$ of $n_u < n_x$ unknowns: $\mathbf{X} = \mathbf{M}(\mathbf{U}, \mathbf{Z})$. Substituting $\mathbf{M}$ into $\mathbf{F}_1$, and defining $\mathbf{H}(\mathbf{U}, \mathbf{Z}) \equiv \mathbf{F}_1(\mathbf{M}(\mathbf{U}, \mathbf{Z}), \mathbf{Z})$, we can rewrite (27) as the reduced system

$$\mathbf{H}(\mathbf{U}, \mathbf{Z}) = 0. \tag{29}$$

For instance, for the Krusell–Smith model from Section 2, $\mathbf{X}_t$ includes capital K_t, returns r_t, and wages w_t, and $\mathbf{F}$ includes asset market equilibrium and the factor demand equations. But we solve out the factor demand equations to write r_t and w_t in terms of K_{t-1}

[19] Sequence-space Jacobians may nevertheless be useful in solving some versions of these models, as recently demonstrated by Fukui (2020) (in a wage-posting model) and Alves (2020) (in a sequential auction framework).

and Z_t in (5) and (6), and writing this solution as the function $\mathbf{M}$, we are left with $\mathbf{U}_t = K_t$, and an $\mathbf{H}$ that includes only asset market equilibrium.

We use the implicit function theorem to solve for $d\mathbf{X}$ in two steps:

$$d\mathbf{U} = -\mathbf{H}_{\mathbf{U}}^{-1}\mathbf{H}_{\mathbf{Z}}\, d\mathbf{Z}, \tag{30}$$

$$d\mathbf{X} = \mathbf{M}_{\mathbf{U}}\, d\mathbf{U} + \mathbf{M}_{\mathbf{Z}}\, d\mathbf{Z} = \mathbf{G}\, d\mathbf{Z}. \tag{31}$$

When the number of unknowns n_u is much smaller than the number of endogenous variables n_x, this is much more efficient than applying the implicit function theorem directly to $\mathbf{F}$.

Calculating Jacobians of $\mathbf{H}$ *and* $\mathbf{M}$. To implement (30) and (31), we need the Jacobians of $\mathbf{H}$ and $\mathbf{M}$. In a heterogeneous-agent model, these functions will include the aggregate actions of agents, for which we can compute the relevant Jacobians using the fake news algorithm from Section 3. We can then combine these Jacobians with the rest of the model using the chain rule.

In models where $\mathbf{H}$ and $\mathbf{M}$ are sufficiently complex, it is helpful to obtain their Jacobians with a more automated approach, rather than applying the chain rule manually as we did in Section 2. In Appendix C.2, we describe how to build up $\mathbf{H}$ and $\mathbf{M}$ as the directed acyclical graph (DAG) of smaller blocks, and in Appendix C.3, we show how to compose the Jacobians of these blocks to efficiently obtain the Jacobians of the model. This modular approach allows us to efficiently handle models with a large number of aggregate equilibrium conditions, such as the two-asset model in Appendix B.3, and we use it to solve all the models in this paper. For instance, Figure 3 shows the DAG representation of the Krusell–Smith model.

Another possibility is to use an off-the-shelf automatic differentiation package. However, directly using such a package on the entire functions $\mathbf{H}$ and $\mathbf{M}$, including the parts that deal with heterogeneous agents, fails to take advantage of the special structure of heterogeneous-agent Jacobians, and can therefore be quite costly.[20] It is far more efficient to use the fake news algorithm to compute Jacobians for the heterogeneous-agent part of the problem, and then supply these Jacobians to the package.

Finally, a simple (but less accurate) option is to numerically differentiate $\mathbf{H}$ and $\mathbf{M}$. As with automatic differentiation, a direct application of numerical differentiation is ineffi-

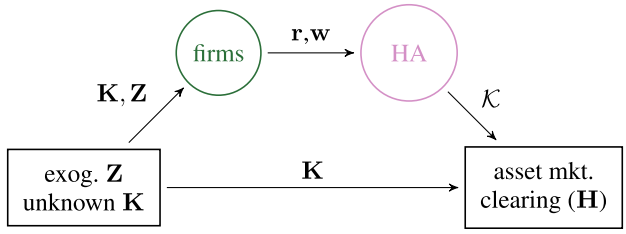

FIGURE 3.—DAG representation of Krusell–Smith economy.

[20]See Ahn, Moll, and Schaab (2018) for an example of directly applying automatic differentiation to the entire $\mathbf{H}$ and $\mathbf{M}$. Effectively, the computer then follows an approach resembling the direct method discussed in Section 3.1. See also Childers (2018) for an application of automatic differentiation to heterogeneous-agent models.

cient, but can be made much faster by replacing the heterogeneous-agent parts of these functions with linearized counterparts obtained using the fake news algorithm.[21]

4.2. *Numerical Accuracy: Equivalence to the Reiter Method*

We now establish that our implementation of the sequence-space Jacobian ("SSJ") method is accurate by comparing the solution it produces to that obtained using the Reiter method.

In principle, the two methods should give the same solution, that is, the first-order solution of the model in aggregates. Indeed, they are both intended to solve to first order the same system of equations, which includes (10)–(12) and additional equations in (27). There are, however, two potential concerns to rule out. First, both our method and Reiter—like all first-order perturbation methods—are subject to error when computing derivatives. Second, rather than solving the true infinite-dimensional system in sequence space, our method truncates sequence-space Jacobians at some high T.[22]

To verify accuracy, we choose as our benchmark the Reiter method with automatic differentiation. Automatic differentiation, unlike numerical differentiation, ensures that there is no approximation error when computing derivatives. We then show that the SSJ method—with the same parameterization on the same grid and $T = 300$, and the fake news algorithm implemented using automatic differentiation—delivers identical impulse responses to Reiter, and that its state-space law of motion is also identical.[23] We find that the SSJ method with numerical differentiation delivers larger but still relatively minor errors. We finally discuss practical considerations in choosing T.

As is well known, the main bottleneck of the Reiter method is that it cannot be used directly with large idiosyncratic state spaces without model reduction (the method scales in the cube of the size of the idiosyncratic state space). For this reason, we restrict our comparison to the Krusell–Smith model and the one-asset HANK model, each computed on a small grid of $n_g = 300$ points (100 asset grid points and 3 income states). We describe our implementation of the Reiter method in Appendix C.6.

Preliminaries: Benchmark Representative-Agent Models. Before proceeding, we first check that our implementation of the SSJ method is accurate for models without heterogeneity. We verify that the linear impulse responses of output to all shocks in the Smets and Wouters (2007) model and in the Herbst and Schorfheide (2015) model—two benchmark models used extensively for estimation in the literature—are identical, to within 5 and 14 digits respectively, to those obtained using the first-order solution from Dynare, which uses standard state-space methods for computation.[24]

[21] For instance, in the Krusell–Smith model, one would rewrite household asset demand as $\mathcal{K} - K_{ss} = \mathcal{J}^{K,w} \cdot (\mathbf{w} - w_{ss}) + \mathcal{J}^{K,r} \cdot (\mathbf{r} - r_{ss})$, using the Jacobians $\mathcal{J}^{K,w}$ and $\mathcal{J}^{K,r}$ calculated with the fake news algorithm.

[22] Recall from equations (10)–(12) that we take as given a discretized model, which we take to be the "true" model. We compare the solution to the Reiter method applied to the same discretized model. If the "true" model is continuous instead, getting to the discretized model in the first place involves some error, but this does not affect the comparison here.

[23] Note that this usage of automatic differentiation in the backward iteration of the fake news algorithm, which is discussed in Section 3.2, is distinct from the usage of automatic differentiation discussed in Section 4.1: the former is to obtain error-free derivatives of v, Λ, and y in (10)–(12), while the latter is to obtain derivatives of H.

[24] Impulse responses and numerical errors are plotted in Appendix E.5.

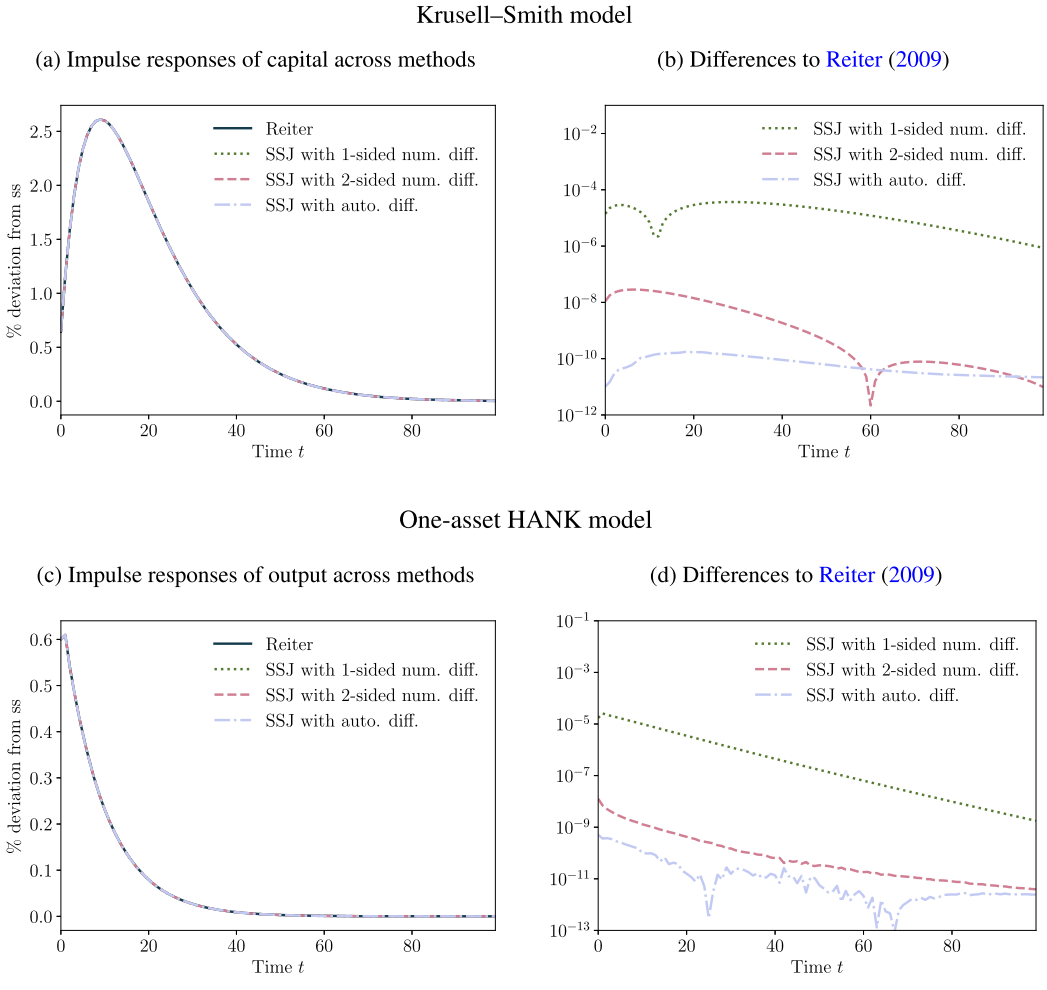

FIGURE 4.—Equivalence between the SSJ and the Reiter (2009) methods.

Accuracy of Impulse Responses. Figure 4 compares the impulse responses from the Reiter method with automatic differentiation, and the impulse responses produced by our SSJ method using the three types of differentiation discussed in Section 3.2. All panels compute impulse responses to a 1% TFP shock with persistence $\rho = 0.9$, and the SSJ truncation horizon is chosen at $T = 300$. The top panels show the impulse response of capital in the Krusell–Smith model. The bottom panels show the impulse response of output in the one-asset HANK model. Panels (a) and (c) plot the impulse responses in levels using all four methods. The impulse responses look visually identical. To get a sense of the differences, panels (b) and (d) plot the absolute value of the differences between the lines in the left panel and the Reiter solution at each t. When solved with automatic differentiation, our method yields essentially the same result as the Reiter solution with automatic differentiation, up to ten digits of accuracy. Applying our method with numerical differentiation predictably introduces a small error, comparable to the errors typically found when implementing the Reiter method with numerical differentiation. Despite this error already being small, one can reduce it significantly at just twice the computational

cost by using two-sided numerical differentiation. This is important because two-sided numerical differentiation is often easier to implement than automatic differentiation in practice.

Accuracy of the State-Space Law of Motion. While comparison of individual impulse responses is a useful proof of accuracy, a more definitive test is to verify that the state-space laws of motion are identical. In Appendix C.7, we show how to recover the state-space law of motion from our sequence-space solution, by using some of the intermediate outputs of the fake news algorithm. Using this method, we compute the matrices describing the state-space law of motion in the Krusell–Smith model and the one-asset HANK model (with automatic differentiation), and we compare these matrices to those from the Reiter method. We find that the sup norm of the difference between these matrices is below 10^{-8} for both models.

Choice of Truncation Horizon T. We have established that our method, for large enough T, delivers the same solution as the Reiter method. In practice, however, a separate computation via the Reiter method is usually not available as a benchmark. In these cases, how can one ensure that T is, in fact, high enough? To answer this question, we now examine the sensitivity of the sequence-space solution to T.

We take as our benchmark the sequence space solution with a very large T ($T = 1000$), well above the horizon required to achieve agreement with the Reiter method in our previous exercise. We then see how the impulse response in the first 100 periods differs from this benchmark as we reduce T. Throughout, we compute Jacobians with one-sided numerical differentiation, since it is the easiest and most commonly used in practice.

Figure 5 performs this exercise for our three models, each in response to a 1% shock to TFP with persistence ρ. In the left panel, $\rho = 0.9$. We see that even for truncation horizons T far shorter than the $T = 300$ used in this paper, the RMSE of the output impulse response dY/Y_{ss} is near zero in both the Krusell–Smith and one-asset HANK models. The two-asset HANK model, on the other hand, only achieves five digits of accuracy by $T = 300$. This is because that model has much greater internal persistence: the magnitude of the underlying output impulse response at $t = 300$ is above $10^{-4}\%$, while it is below $10^{-9}\%$ for the two other models. (By that point, the shock itself is below $10^{-13}\%$.)

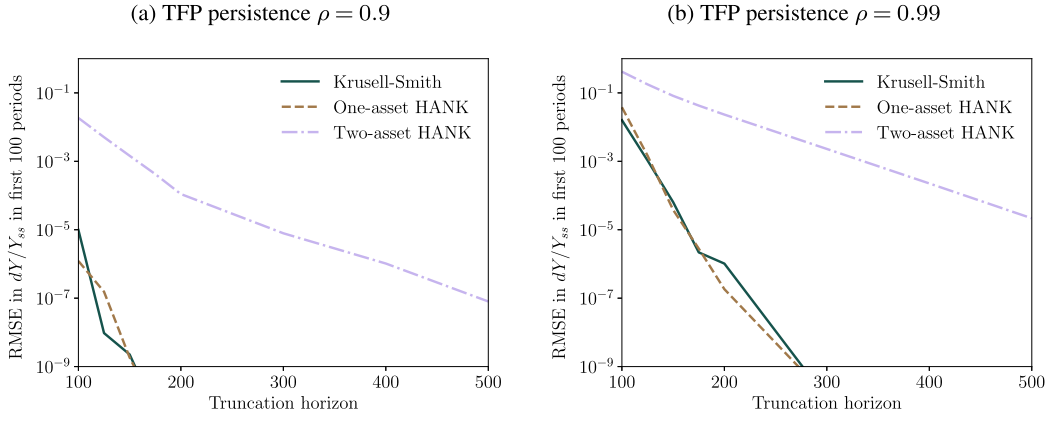

FIGURE 5.—Impulse response error (relative to $T = 1000$) as a function of the truncation horizon T.

The right panel looks at a more extreme case, with $\rho = 0.99$. Here, the shock at $t = 300$ remains at 5% of its level on impact. Now the two-asset HANK model achieves less than three digits of accuracy even with $T = 300$, and about five digits of accuracy with $T = 500$. This indicates the importance of a high T when dealing with highly persistent shocks, especially in models with high internal persistence.[25]

Overall, to be sure that the truncation horizon is long enough, it is most important to ensure that both the shock itself and the endogenous impulse response—which may feature some internal persistence—are near zero by T. An additional check is to make sure that changing T to a higher value does not change the impulse response: as Figure 5 indicates, when T is not yet high enough to deliver accuracy, the results are sensitive to changes in T. These two simple checks ensure that one has minimized truncation error, leaving numerical differentiation as the only possible remaining source of error relative to the true first-order solution of the model in aggregates.

5. APPLICATION TO ESTIMATION

We now discuss how to use the sequence-space Jacobian method to estimate models on time-series data. This application uses the equivalence of impulse responses with the moving-average (MA) representation of the model with aggregate shocks. This equivalence, in turn, follows immediately from the certainty equivalence property of first-order perturbation methods such as ours (see, e.g., Simon (1956), Theil (1957), Judd and Guu (1993), and Boppart, Krusell, and Mitman (2018)).

We assume that the exogenous shocks follow independent moving-average processes, that is, the vector-valued stochastic process $d\tilde{\mathbf{Z}}$ is given by

$$d\tilde{\mathbf{Z}}_t = \sum_{s=0}^{\infty} d\mathbf{Z}_s \boldsymbol{\epsilon}_{t-s}, \tag{32}$$

where $\boldsymbol{\epsilon}_t$ is an n_z vector of mutually i.i.d. standard normally distributed innovations, and $\{d\mathbf{Z}_{t+s}\}_s$ are the impulse responses to a unit innovation to $\boldsymbol{\epsilon}_t$.

Equation (28) tells us that the impulse responses of endogenous variables $d\mathbf{X}$ can be obtained by simple matrix multiplication of the impulse of shocks $d\mathbf{Z}$ with the general equilibrium Jacobian $\mathbf{G}$. Certainty equivalence then implies that the stochastic process $d\tilde{\mathbf{X}}$ follows the moving-average process

$$d\tilde{\mathbf{X}}_t = \sum_{s=0}^{T-1} d\mathbf{X}_s \boldsymbol{\epsilon}_{t-s}. \tag{33}$$

The rapid computation of this MA$(T-1)$ representation is the foundation of our applications in this section, which will build up to likelihood-based estimation of our three models.

[25] Interestingly, the error in the first 100 periods in the other two models is below 10^{-9} with $T = 300$, in spite of the shock's persistence. Of course, there is still error near $t = 300$, as is inevitable when the shock has not died out by the truncation horizon, but this error does not propagate backward in these models to nearly the same extent. This lack of backward propagation is related to the weaker internal persistence in these models relative to the two-asset HANK model.

(a) Simulation of various series X (b) Corr(dX_{t+l}, dZ_t) for various series X

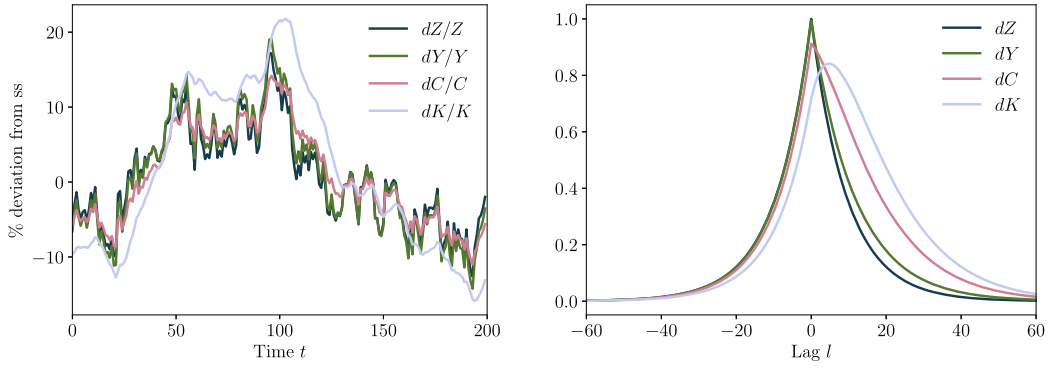

FIGURE 6.—Simulations and second moments of the Krusell and Smith (1998) model for AR(1) TFP, $\rho = 0.9$.

5.1. *Simulation*

As pointed out by Boppart, Krusell, and Mitman (2018), the formulation in equation (33) is useful to simulate sample paths for aggregate variables generated by any model, including a heterogeneous-agent model. Assume impulse responses $d\mathbf{X}$ have been computed with truncation horizon T. Then, a procedure to simulate a random sample path of $d\tilde{\mathbf{X}}$ is as follows: first, draw paths for the shock innovations, that is, a sequence $\{\boldsymbol{\epsilon}_t\}$ up to a large horizon $\mathbb{T}$. Second, evaluate (33) for each t. Finally, discard the first T elements. This procedure generates a random sample path of length $\mathbb{T} - T$.[26] Panel (a) of Figure 6 presents an example of such simulations for the Krusell–Smith model with AR(1) TFP shocks.[27]

Table I shows that, given the $\mathbf{G}$ matrices, this simulation procedure is extremely fast in practice: to draw sample paths of length 100,000 for the observables used in the estimation of our four main models at their posterior modes in Section 5.4, we only need 5 ms for the Krusell–Smith model (one observable, one shock), 22 ms for the one-asset HANK model (three observables, three shocks), and 105 ms for the two-asset HANK model (seven observables, seven shocks).

One use of these simulated sample paths, as Boppart, Krusell, and Mitman (2018) showed, is to compute the second moments of outcomes—their variances and covariances, at various lags and leads. In the next section, however, we will instead discuss a more efficient, analytical way of computing these moments, based directly on the impulse responses $d\mathbf{X}$.

5.2. *Analytical Second Moments*

The autocovariances of the vector-valued stochastic process $d\tilde{\mathbf{X}}_t$ with MA coefficients $d\mathbf{X}$ are given by the standard expression (see, for instance, Box and Jenkins (1970) and

[26] In Appendix E.3, we explain how to extend this procedure to simulate panels of individuals.

[27] For this simulation, we assume an AR(1) process for TFP with persistence $\rho = 0.9$, and innovations with standard deviation of $\sigma = 0.02$. We set $T = 300$ and $\mathbb{T} = 500$, so there are 200 periods of observation.

Hamilton (1994)):

$$\mathrm{Cov}(d\tilde{\mathbf{X}}_t, d\tilde{\mathbf{X}}_{t'}) = \sum_{s=0}^{T-1-(t'-t)} (d\mathbf{X}_s)(d\mathbf{X}_{s+t'-t})'. \tag{34}$$

The covariance in (34) only depends on the distance $t' - t$, not on t and t' separately.

In panel (b) of Figure 6, we provide an illustration of these second moments for the parameterization of the stochastic Krusell–Smith model simulated in panel (a). The figure shows the correlations of productivity, output, consumption, and capital with the underlying productivity process, at various lags. The figure shows that capital and consumption—and to a much lesser extent, output—tend to lag productivity. This reflects the typical transmission mechanism of TFP shocks in RBC models.

As Table III reveals, it is very fast to calculate autocovariances in this way: for our estimation exercises of Section 5.4, moving from the MA($T-1$) representation to a full set of autocovariances, which are stacked in constructing the matrix $\mathbf{V}$, only takes between 0.4 and 0.7 milliseconds.[28] These autocovariances can be used directly to calibrate or estimate a model—as in the simulated method of moments, but without the need for explicit simulation.[29] Alternatively, they can be used to evaluate the likelihood function, as an input to likelihood-based estimation on time-series data. This is where we turn next.

5.3. *Evaluating the Likelihood Function*

The typical approach to likelihood-based estimation in the DSGE literature is to compute the likelihood by applying the Kalman filter to the model's state-space representation (see, e.g., Smets and Wouters (2007), An and Schorfheide (2007), Herbst and Schorfheide (2015), and Fernández-Villaverde, Rubio-Ramírez, and Schorfheide (2016)). This approach is appropriate for models with small state spaces. With the large state spaces that characterize heterogeneous-agent models, however, evaluating the likelihood in this fashion can be prohibitively slow.

We now suggest an alternative approach: to use the MA representation provided by the sequence-space Jacobian method to rapidly compute (and recompute) the likelihood. The idea of using the MA representation of a DSGE model directly to calculate the likelihood goes back to at least Hansen and Sargent (1981). There are multiple ways to perform this calculation. The approach we employ in our application builds directly on the analytical moments from the previous section.[30] Let

$$d\tilde{\mathbf{X}}_t^{\mathrm{obs}} = B\, d\tilde{\mathbf{X}}_t + \mathbf{u}_t \tag{35}$$

denote the vector of n_{obs} observables whose likelihood we would like to determine.[31] Here $\{\mathbf{u}_t\}$ is i.i.d. normal with mean 0 and covariance matrix Σ_u, and B is an $n_{\mathrm{obs}} \times n_x$ matrix.

[28] This is facilitated by using the fast Fourier transform to calculate (34) in a highly efficient way, a process that we describe in Appendix E.4.

[29] For recent examples of this approach to estimation, see Auclert and Mitman (2020) and Bardóczy (2020). For a previous instance of an analytical approach to calculating second moments from a heterogeneous-agent model, see Harmenberg and Sievertsen (2017).

[30] Recent papers in the DSGE literature that use the same approach include Mankiw, Gregory, and Reis (2007) and Schmitt-Grohé and Uribe (2010).

[31] These may include moments of micro data (if we interpret $\mathbf{u}_t$ as sampling error), since we can construct model impulse responses for such moments using our extended methods from Appendices A.1 and A.2. More comprehensively integrating micro data into time-series estimation requires other methods. For promising work along these lines, see Chang, Chen, and Schorfheide (2018) and Plagborg-Møller and Liu (2019).

Since $d\tilde{\mathbf{X}}_t^{\text{obs}}$ is a linear combination of the $\boldsymbol{\epsilon}_t$ and $\mathbf{u}_t$ terms, it has a multivariate normal distribution. Moreover, its second moments are a simple linear transformation of those of $d\tilde{\mathbf{X}}_t$:

$$\operatorname{Cov}\left(d\tilde{\mathbf{X}}_t^{\text{obs}}, d\tilde{\mathbf{X}}_{t'}^{\text{obs}}\right) = 1_{t=t'} \cdot \boldsymbol{\Sigma}_{\mathbf{u}} + B \operatorname{Cov}(d\tilde{\mathbf{X}}_t, d\tilde{\mathbf{X}}_{t'}) B'. \tag{36}$$

We stack these covariances into a large symmetric $n_{\text{obs}} T_{\text{obs}} \times n_{\text{obs}} T_{\text{obs}}$ matrix $\mathbf{V}$, where T_{obs} is the number of time periods in our data.[32] The log-likelihood function is then the conventional log multivariate density. Dropping the constant term, it can be expressed as a function of the observed data $d\tilde{\mathbf{X}}^{\text{obs}} = (d\tilde{\mathbf{X}}_t^{\text{obs}})$ (stacked as an $n_{\text{obs}} T_{\text{obs}}$-dimensional vector) as

$$\mathcal{L} = -\frac{1}{2} \log\det \mathbf{V} - \frac{1}{2} \left[d\tilde{\mathbf{X}}^{\text{obs}}\right]' \mathbf{V}^{-1} \left[d\tilde{\mathbf{X}}^{\text{obs}}\right]. \tag{37}$$

We evaluate this expression by performing a Cholesky decomposition of $\mathbf{V}$, from which we can quickly calculate both the log determinant $\log\det \mathbf{V}$ and the quadratic form $[d\tilde{\mathbf{X}}^{\text{obs}}]' \mathbf{V}^{-1} [d\tilde{\mathbf{X}}^{\text{obs}}]$.[33] Table III reveals that this is quite efficient in our applications: calculating $\mathcal{L}$ takes about 2 milliseconds or less in all except the two-asset HANK, where it takes about 12 milliseconds.

A weakness of this approach is that the Cholesky decomposition of $\mathbf{V}$ requires time proportional to $n_{\text{obs}}^3 T_{\text{obs}}^3$. As the number of time-series observations T_{obs} grows, this can become quite costly.[34] An alternative that scales better with T_{obs} is to use the Whittle approximation to the likelihood, as in Hansen and Sargent (1981) and Plagborg-Møller (2019), which can be efficiently calculated using the Fast Fourier Transform.

Another approach is to construct a state-space system from the MA representation, including the most recent T realizations of the innovations $\boldsymbol{\epsilon}_t$, and then apply the Kalman filter. This system is distinct from the usual state-space one, and does not scale with the underlying heterogeneity—but since its size is proportional to the truncation horizon T, it is often large enough in our applications that applying the Kalman filter is costly. Still, this approach has a number of advantages: for instance, its cost only scales linearly in T_{obs}, and if desired we can apply the Kalman smoother to do inference on shocks.

5.4. *Bayesian Estimation*

In this section, we perform a Bayesian estimation of macro parameters for our three example economies. Our primary objective is to illustrate that, by reusing Jacobians, this can be done very efficiently with the SSJ method. We first estimate the posterior mode, and then use a standard Markov chain Monte Carlo method (Random Walk Metropolis–Hastings, RWMH) to trace out the shape of the posterior distribution, as described in Herbst and Schorfheide (2015). We leave a detailed understanding of the economics behind the estimation results to future research.

[32] Missing or mixed-frequency data can be easily accommodated by replacing the B in (35) with a time-specific B_t, which can have a time-varying number of rows. The second term on the right in (36) then becomes $B_t \operatorname{Cov}(d\tilde{\mathbf{X}}_t, d\tilde{\mathbf{X}}_{t'}) B_{t'}'$.

[33] We provide an accuracy check of our implementation of (37) by using it to find the posterior modes of the Herbst and Schorfheide (2015) and the Smets and Wouters (2007) models, on their original data sets. Table F.1 in Appendix F.1 shows that the modes are numerically identical to those obtained in Dynare given the state-space formulations of these models.

[34] One relatively minor modification, which exploits the block Toeplitz structure of $\mathbf{V}$, is to use Levinson recursion instead of the Cholesky decomposition (e.g., Meyer-Gohde (2010)). Asymptotically, this scales with T_{obs}^2 instead, although for our applications it did not deliver a major improvement.

Reusing Jacobians. Likelihood-based estimation involves computing the likelihood function many times for different parameters. In our case, given equation (37), this requires computing the covariance matrix of model observations $\mathbf{V}$ for each parameter draw, which in turn requires computing the impulse responses $d\mathbf{X}$. Our key innovation is to make the repeated computation of $d\mathbf{X}$ very efficient by reusing Jacobians. The benefits of this procedure, however, depend on which parameters we are estimating.

Consider first the estimation of the parameters of shock processes. In this case, the matrix $\mathbf{G}$ in equation (31) is unchanged across parameter draws, since these parameters only change the vector $d\mathbf{Z}$. Hence, it is sufficient to compute $\mathbf{G}$ once, and then for each parameter draw form $d\mathbf{X}$, $\mathbf{V}$, and $\mathcal{L}$ without re-solving the model. This separation constitutes a clear advantage of our sequence-space approach relative to a state-space approach to estimation.

Next, consider the estimation of parameters that do not change the steady state of the heterogeneous-agent problem. This includes parameters that govern price stickiness, capital adjustment costs, or monetary policy rules. These parameters also do not affect the Jacobian of the heterogeneous-agent problem. Hence, in the construction of the total model Jacobian in equation (56), these Jacobians can be held fixed at their initial value.[35] Since heterogeneous-agent Jacobians are by far the most time-consuming step in obtaining $\mathbf{G}$ (see Table I), this is still very fast.

Finally, consider estimating parameters that do change the steady state of the heterogeneous-agent problem. There, the Jacobian of that problem needs to be recomputed for each new draw of parameters, together with the steady state. While the fake news algorithm speeds up Jacobian computation considerably, the additional time cost of re-evaluating the steady state on each draw remains substantial, and we do not pursue this type of estimation here.[36]

Priors, Data, and Estimation. We now proceed to our main estimation exercise. Across all models, we assume the following prior distributions. We assume that the priors for the standard deviations of all shocks are Inverse-Gamma distributed with mean 0.4 and standard deviation 4. We assume that the priors for persistence parameters are Beta distributed with mean 0.5 and standard deviation 0.2. We also assume no measurement error, $\Sigma_{\mathbf{u}} = 0$. We describe the priors of model-specific parameters below. We search for the posterior mode using a standard optimization routine, starting with the prior mode as our initial guess.[37] We run a standard RWMH in which the proposal distribution is a multivariate normal with variance equal to the inverse Hessian at the posterior mode, scaled by a factor c that is adjusted to get an acceptance rate around 25%.[38] We simulate the Markov chain for 100,000 draws, discarding the first 50,000.

[35]This statement is true, more generally, of the Jacobian of any block in the DAG whose parameters do not change.

[36]In the literature, Winberry (2018), Auclert, Rognlie, and Straub (2020), and Bayer, Born, and Luetticke (2020) all calibrated the steady-state micro parameters governing the heterogeneous-agent problem, and used time-series data only to estimate macro parameters, as we do here. In recent work, Acharya, Cai, Del Negro, Dogra, Matlin, and Sarfati (2020) used time-series data to also estimate micro parameters, with sequential Monte Carlo methods to speed up estimation. Also see Plagborg-Møller and Liu (2019), who estimated micro parameters using a mix of micro and macro data.

[37]Specifically, we use the SciPy implementation of L-BFGS-B, imposing some non-binding bounds to guide the routine away from poorly-behaved regions of the parameter space.

[38]One simple improvement, which we do not attempt, might be to use a proposal distribution where a positive probability of draws only changes the parameters of shock processes, not other parameters. Since we can re-use $\mathbf{G}$, calculating the likelihood for these draws would be much faster.

For each model, we use the same U.S. data series as those used in Smets and Wouters (2007), over the same sample period (1966:1–2004:4). We linearly de-trend the logs of all growing variables (output, consumption, investment, wages, hours) and take out the sample means of inflation and nominal interest rates. The individual models are then estimated as follows.

Krusell–Smith Model. We estimate our Krusell and Smith (1998) model with a single shock, TFP, and a single time series $\{dX_t^{\text{obs}}\}$, output. We assume that TFP shocks follow an ARMA(1, 1) process, $(1-\rho L)\, d\tilde{Z}_t = (1-\theta L)\sigma\epsilon_t$, where L denotes the lag operator. We estimate the roots ρ, θ as well as the standard deviation σ. Table F.2 in Appendix F shows the estimates, finding a persistent AR root $\rho \approx 0.9$, as well as a relatively small MA component $\theta \approx 0.03$. Recursive means and univariate plots of the posterior distribution sampled with the RWMH algorithm suggest that the Markov chain has converged and the posterior distribution is well behaved.

One-Asset HANK Model. We estimate our one-asset HANK model both with only shock parameters, and with shock and model parameters together. In both cases, we use three shocks (monetary policy shocks, government spending shocks, and price markup shocks) and three time series (output, inflation, and nominal interest rates). Each shock is modeled as an AR(1) with its own standard deviation and persistence. Thus, there are six shock parameters for this model. The first four posterior columns in Table F.3 in Appendix F show our estimates when only estimating those shock parameters; we find persistent government spending shock and price markup shocks, while monetary policy shocks are less so. The last four posterior columns in this table report the estimated shock and model parameters in the joint estimation. We find a Taylor coefficient ϕ of around 1.3, a modest responsiveness of the Taylor rule to output $\phi_y \approx 0.13$, and a Phillips curve slope parameter κ around 0.14. These are standard values in the literature. Again, recursive means and posterior distribution plots suggest good convergence properties for the RWMH algorithm.

Two-Asset HANK Model. We add all seven shocks from Smets and Wouters (2007) to the two-asset model: shocks to TFP, government spending, monetary policy, price and wage markups. The two exceptions are that we use discount factor shocks rather than "risk premium" shocks (both shock the Euler equation and are thus very similar), and we shock firms' first-order conditions for capital instead of using investment-specific technology shocks.[39] We estimate the parameters of these seven shock processes using time-series data on output, consumption, investment, hours, wages, nominal interest rates and price inflation. As with the one-asset model, we estimate two versions of the model, one with only shock parameters and one with shock and model parameters (Table F.4 in Appendix F). Compared to the one-asset model, we find here somewhat less responsive coefficients of the Taylor rule on inflation and output at the mode, but also a much wider 90% credible interval. We also find smaller Phillips curve slope parameters κ^p, κ^w. We also estimate the degree of capital adjustment costs ϵ_I and find it to be in line with standard estimates from the literature. The evolution of the recursive means across the 150,000 non-discarded draws, as well as the estimated posterior distributions, suggest good convergence properties when we only estimate shocks, but less stability when estimating both

[39] Investment-specific technology shocks are known to have counterfactual implications for the relative price of investment—see, for instance, Justiniano, Primiceri, and Tambalotti (2011).

TABLE III
ESTIMATION TIMES

	Krusell–Smith	One-Asset HANK		Two-Asset HANK	
	Shocks	Shocks	Model + Shocks	Shocks	Model + Shocks
Single likelihood evaluation	**0.639 ms**	**2.353 ms**	**56.001 ms**	**13.992 ms**	**227.245 ms**
step 1 (MA)	0.015 ms	0.091 ms	53.686 ms	1.139 ms	214.396 ms
step 2 (autocovariances)	0.041 ms	0.144 ms	0.146 ms	0.706 ms	0.712 ms
step 3 (log-likelihood)	0.582 ms	2.117 ms	2.169 ms	12.148 ms	12.137 ms
Posterior mode optimization	**0.06 s**	**0.66 s**	**13.95 s**	**16.22 s**	**522.03 s**
no. of evaluations	81	237	580	1094	6560
Random Walk Metropolis–Hastings	**132.40 s**	**568.42 s**	**11,217.00 s**	**2899.58 s**	**42,563.90 s**
no. of evaluations	200,000	200,000	200,000	200,000	200,000
acceptance rate	0.253	0.248	0.253	0.255	0.241
scaling factor c	2.50	1.10	0.65	0.40	0.10
No. of shocks	1	3	3	7	7
No. of estimated shock parameters	3	6	6	14	14
No. of estimated model parameters	0	0	3	0	5
Total no. of estimated parameters	3	6	9	14	19

shocks and parameters. This could be due to the fact that the model is not designed explicitly to fit the hump shapes in the time series; see Auclert, Rognlie, and Straub (2020) for a model that addresses this shortcoming.

Estimation Times. Table III lists computing times for each of our five estimation exercises, including times for each likelihood evaluation and their breakdown into the three steps described in Section 5.3.

Once the **G** matrix is computed (Table C.1), the Krusell–Smith model's likelihood can be evaluated in less than one millisecond, and the posterior mode can be found in around 60 milliseconds. The entire RWMH estimation takes just over two minutes. We attain similar speeds estimating the shock processes for the one-asset HANK model (just under 10 minutes for RWMH). Since we allow for seven shocks when estimating the two-asset HANK model, estimating the parameters of these shock processes is somewhat slower than in the other two models; this has nothing to do with the complexity or micro heterogeneity of the two-asset model. Still, a single likelihood evaluation only takes a few milliseconds, the posterior mode is found in a few seconds, and RWMH estimation takes about 50 minutes.

When model parameters are also estimated, the likelihood takes a bit longer to be re-evaluated. This is entirely due to step 1—the computation of impulse responses. The single likelihood evaluation for the two-asset model, for instance, takes 227 ms rather than 14 ms when model parameters change, and finding the posterior mode takes less than 9 minutes. Running RWMH with 200,000 evaluations on the two-asset model when estimating 19 shock processes and model parameters takes less than 12 hours. To the best of our knowledge, these are much faster speeds for estimation of such models than what any other method has been able to achieve at a comparable level of accuracy.

Our main contribution in this section, the idea of reusing Jacobians, is essential to achieving these speeds. To illustrate this, observe that re-evaluating the heterogeneous-agent Jacobian 200,000 times for the two-asset model would take about 8 full days with

our fake news algorithm (approximately 3.5 s per evaluation), and about 6 years with the direct algorithm (approximately 950 s per evaluation).

6. APPLICATION TO NONLINEAR PERFECT-FORESIGHT TRANSITIONS

We now discuss how to use sequence-space Jacobians to obtain nonlinear solutions to equation (27). These solutions are the nonlinear perfect-foresight impulse responses to unexpected shocks perturbing the aggregate steady state at date 0 (sometimes called "MIT shocks"). In the literature, these are used by researchers to explore size dependence and sign asymmetries (see, e.g., Kaplan and Violante (2018) for fiscal policy and Bayer, Guerrieri, Lorenzoni, and Vavra (2018) for house price changes), and to simulate transitions between two steady states in applications that involve long-term changes (see, e.g., Heathcote, Storesletten, and Violante (2010) for rising inequality and Krueger and Ludwig (2007) for demographic change). Recently, Boppart, Krusell, and Mitman (2018) have also suggested examining the extent of size dependence in these shocks as a test of how closely the first-order aggregate perturbation matches the nonlinear solution with aggregate risk.

To find the $\mathbf{U}$ that solves $\mathbf{H}(\mathbf{U}, \mathbf{Z}) = 0$ for a given $\mathbf{Z}$, truncated to some T, we use the following iterative procedure. First, starting from $j = 0$, guess a path $\mathbf{U}^0$ (typically, $\mathbf{U}^0 = \mathbf{U}_{ss}$). Second, calculate $\mathbf{H}(\mathbf{U}^j, \mathbf{Z})$. Third, form the $j+1$ guess using

$$\mathbf{U}^{j+1} = \mathbf{U}^j - \left[\mathbf{H}_{\mathbf{U}}(\mathbf{U}_{ss}, \mathbf{Z}_{ss})\right]^{-1} \mathbf{H}\left(\mathbf{U}^j, \mathbf{Z}\right). \tag{38}$$

This algorithm falls in the class of quasi-Newton methods,[40] since the steady-state sequence-space Jacobian $\mathbf{H}_{\mathbf{U}}(\mathbf{U}_{ss}, \mathbf{Z}_{ss})$ is used instead of the actual Jacobian $\mathbf{H}_{\mathbf{U}}(\mathbf{U}^j, \mathbf{Z})$.[41] Once we obtain $\mathbf{U}$, we can compute the full set of endogenous variables directly from $\mathbf{X} = \mathbf{M}(\mathbf{U}, \mathbf{Z})$. We illustrate this method using our two-asset HANK model in two ways.

Nonlinear Impulse Responses. Panel (a) of Figure 7 shows three impulse responses of consumption in the two-asset HANK model in response to monetary policy shock with quarterly persistence $\rho = 0.6$. Two are the linear and nonlinear impulse responses to a -5pp shock to the Taylor rule, and the other is the nonlinear impulse response to a -1pp shock, scaled up by a factor of 5. The linear and scaled-up nonlinear impulse responses are almost identical, indicating that linearity is an accurate assumption for -1pp shocks. The nonlinear impulse response to the -5pp shock is visibly a bit smaller than the other two, but still similar: 0.81% on impact, rather than 0.86%. This similar response, despite the extreme size of the monetary shock, suggests that nonlinearities in the household model—such as large shocks moving households away from their borrowing constraints—do not play an important role for plausibly-sized shocks.

The algorithm above converges to $|\mathbf{H}| < 10^{-8}$ in 13 iterations for the -5pp shock, and 5 iterations for the -1pp shock. By contrast, methods that rely on ad hoc adjustment criteria often require hundreds of iterations before convergence.

[40] This idea of Newton's method to compute nonlinear impulse responses dates back to Laffargue (1990), Boucekkine (1995), and Juillard (1996). For heterogeneous-agent models, previous versions of the method in (38) were implemented by approximating the $\mathbf{H}_{\mathbf{U}}(\mathbf{U}_{ss}, \mathbf{Z}_{ss})$ matrix: see, among others, Auclert and Rognlie (2018), Straub (2017), and Koby and Wolf (2020). For an example using automatic differentiation to obtain $\mathbf{H}_{\mathbf{U}}(\mathbf{U}_{ss}, \mathbf{Z}_{ss})$, see Ahn, Moll, and Schaab (2018).

[41] One alternative is to build an approximation to $\mathbf{H}_{\mathbf{U}}(\mathbf{U}^j, \mathbf{Z})$ for each new guess $\mathbf{U}^j$, holding heterogeneous-agent Jacobians constant at their steady-state values but using exact Jacobians elsewhere. This is useful when there are substantial nonlinearities originating outside the heterogeneous-agent block.

(a) Consumption after shocks to Taylor rule

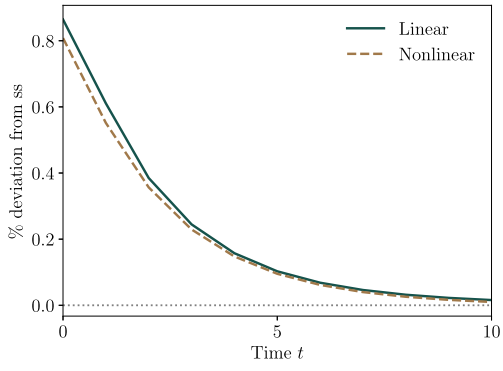

(b) Transition after a 1% permanent TFP shock

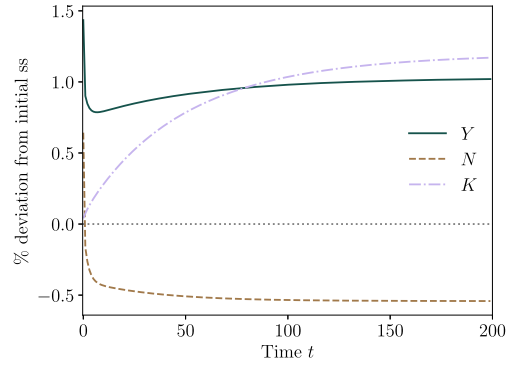

FIGURE 7.—Nonlinear impulse responses and transitional dynamics for the two-asset HANK model.

In Table I, we use the algorithm to compute nonlinear impulse responses for all four of our models, and report the time this requires, which ranges from 0.32 s for Krusell–Smith to 15 s for two-asset HANK. (For comparability, these numbers are for a 1% shock to TFP, which is available in every model.)

Transition to a New Steady State. We can use this algorithm to compute the response to a permanent shock. Here, it is important to use the Jacobian $\mathbf{H}_{\mathbf{U}}(\mathbf{U}_{ss}, \mathbf{Z}_{ss})$ around the terminal steady state. For example, panel (b) of Figure 7 reports the nonlinear transition, starting from the initial steady state of our two-asset HANK model, to a one-time permanent shock of 1% to TFP. In this example, it takes 7 iterations to reach $|\mathbf{H}| < 10^{-8}$.

7. CONCLUSION

This paper presents a highly efficient method for computing heterogeneous-agent models. The core idea is that *sequence-space Jacobians* are sufficient statistics that summarize all we need to know about the heterogeneity in order to determine general equilibrium dynamics, to first order with respect to aggregate shocks. Our main contribution is a fast algorithm for computing the Jacobians of heterogeneous-agent problems. We combine this algorithm with a systematic method for computing model Jacobians and linearized impulse responses. We apply these objects to estimate models with high-dimensional state spaces, and compute their nonlinear transitional dynamics.

Our methods allow us to find the posterior mode of a two-asset HANK model in under ten minutes and trace its posterior distribution with MCMC in under twelve hours, estimation times that had so far been out of reach for the literature. We hope that they will prove useful to solve and estimate other heterogeneous-agent models and facilitate new developments in the field.

REFERENCES

ACHARYA, S., M. D. CAI, M. DEL NEGRO, K. DOGRA, E. MATLIN, AND R. SARFATI (2020): "Estimating HANK: Macro Time Series and Micro Moments," Manuscript. [2401]

AHN, S., G. KAPLAN, B. MOLL, T. WINBERRY, AND C. WOLF (2018): "When Inequality Matters for Macro and Macro Matters for Inequality," *NBER Macroeconomics Annual*, 32 (1), 1–75. [2379,2387]

AHN, S., B. MOLL, AND A. SCHAAB (2018): "Huggett Model: Transition Dynamics, Newton Method Using @myAD," Available at https://benjaminmoll.com/wp-content/uploads/2020/06/huggett_newton_myAD.m. [2393,2404]

ALGAN, Y., O. ALLAIS, AND W. J. DEN HAAN (2010): "Solving the Incomplete Markets Model With Aggregate Uncertainty Using Parameterized Cross-Sectional Distributions," *Journal of Economic Dynamics and Control*, 34 (1), 59–68. [2391]

ALGAN, Y., O. ALLAIS, W. J. DEN HAAN, AND P. RENDAHL (2014): "Chapter 6—Solving and Simulating Models With Heterogeneous Agents and Aggregate Uncertainty," in *Handbook of Computational Economics*, Vol. 3, ed. by K. Schmedders and K. L. Judd. Elsevier, 277–324. [2378]

ALVES, F. (2020): "Job Ladder and Business Cycles," Job Market Paper, New York University. [2392]

AN, S., AND F. SCHORFHEIDE (2007): "Bayesian Analysis of DSGE Models," *Econometric Reviews*, 26, 113–172. [2399]

AUCLERT, A., AND K. MITMAN (2020): "Consumer Bankruptcy as Aggregate Demand Management," Manuscript. [2399]

AUCLERT, A., AND M. ROGNLIE (2018): "Inequality and Aggregate Demand," Working Paper 24280, National Bureau of Economic Research. [2404]

AUCLERT, A., B. BARDÓCZY, M. ROGNLIE, AND L. STRAUB (2019): "Using the Sequence-Space Jacobian to Solve and Estimate Heterogeneous-Agent Models," Working Paper 26123, National Bureau of Economic Research. [2389]

——— (2021): "Supplement to 'Using the Sequence-Space Jacobian to Solve and Estimate Heterogeneous-Agent Models'," *Econometrica Supplemental Material*, 89, https://doi.org/10.3982/ECTA17434. [2380]

AUCLERT, A., M. ROGNLIE, AND L. STRAUB (2018): "The Intertemporal Keynesian Cross," Working Paper 25020, National Bureau of Economic Research. [2391]

——— (2020): "Micro Jumps, Macro Humps: Monetary Policy and Business Cycles in an Estimated HANK Model," Working Paper 26647, National Bureau of Economic Research. [2401,2403]

BARDÓCZY, B. (2020): "Spousal Insurance and the Amplification of Business Cycles," Job Market Paper, Northwestern University. [2399]

BAYER, C., AND R. LUETTICKE (2020): "Solving Discrete Time Heterogeneous Agent Models With Aggregate Risk and Many Idiosyncratic States by Perturbation," *Quantitative Economics*, 11 (4), 1253–1288. [2379]

BAYER, C., B. BORN, AND R. LUETTICKE (2020): "Shocks, Frictions, and Inequality in US Business Cycles," Manuscript. [2401]

BAYER, C., V. GUERRIERI, G. LORENZONI, AND J. VAVRA (2018): "House Prices and Consumer Spending," *Review of Economic Studies*, 85 (3), 1502–1542. [2404]

BOPPART, T., P. KRUSELL, AND K. MITMAN (2018): "Exploiting MIT Shocks in Heterogeneous-Agent Economies: The Impulse Response as a Numerical Derivative," *Journal of Economic Dynamics and Control*, 89, 68–92. [2376,2377,2379,2397,2398,2404]

BOUCEKKINE, R. (1995): "An Alternative Methodology for Solving Nonlinear Forward-Looking Models," *Journal of Economic Dynamics and Control*, 19 (4), 711–734. [2404]

BOX, G. E. P., AND G. M. JENKINS (1970): *Time Series Analysis: Forecasting and Control*. San Francisco: Holden-Day. [2398]

BRUMM, J., AND S. SCHEIDEGGER (2017): "Using Adaptive Sparse Grids to Solve High-Dimensional Dynamic Models," *Econometrica*, 85 (5), 1575–1612. [2378]

BURDETT, K., AND D. T. MORTENSEN (1998): "Wage Differentials, Employer Size, and Unemployment," *International Economic Review*, 39 (2), 257–273. [2391]

CARROLL, C. D. (2006): "The Method of Endogenous Gridpoints for Solving Dynamic Stochastic Optimization Problems," *Economics Letters*, 91 (3), 312–320. [2384]

CHANG, M., X. CHEN, AND F. SCHORFHEIDE (2018): "Heterogeneity and Aggregate Fluctuations," Manuscript. [2399]

CHANG, Y., AND S.-B. KIM (2007): "Heterogeneity and Aggregation: Implications for Labor-Market Fluctuations," *American Economic Review*, 97 (5), 1939–1956. [2391]

CHILDERS, D. (2018): "Automated Solution of Heterogeneous Agent Models," Manuscript. [2393]

CHRISTIANO, L., C. L. ILUT, R. MOTTO, AND M. ROSTAGNO (2010): "Monetary Policy and Stock Market Booms," in *Jackson Hole Symposium Proceedings*. [2386]

DE NARDI, M. (2004): "Wealth Inequality and Intergenerational Links," *Review of Economic Studies*, 71 (3), 743–768. [2391]

DEN HAAN, W. J. (1997): "Solving Dynamic Models With Aggregate Shocks and Heterogeneous Agents," *Macroeconomic Dynamics*, 1 (2), 355–386. [2378]

FERNÁNDEZ-VILLAVERDE, S. HURTADO, AND G. NUÑO (2019): "Financial Frictions and the Wealth Distribution," Working Paper 26302, National Bureau of Economic Research. [2378]

FERNÁNDEZ-VILLAVERDE, J., J. F. RUBIO-RAMÍREZ, AND F. SCHORFHEIDE (2016): "Chapter 9—Solution and Estimation Methods for DSGE Models," in *Handbook of Macroeconomics*, Vol. 2, ed. by J. B. Taylor and H. Uhlig. Elsevier, 527–724. [2379,2399]

FUKUI, M. (2020): "A Theory of Wage Rigidity and Unemployment Fluctuations With on-the-Job Search," Job Market Paper, Massachusetts Institute of Technology. [2392]

GOLOSOV, M., AND R. E. LUCAS (2007): "Menu Costs and Phillips Curves," *Journal of Political Economy*, 115 (2), 171–199. [2391]

GORNEMANN, N., K. KUESTER, AND M. NAKAJIMA (2016): "Doves for the Rich, Hawks for the Poor? Distributional Consequences of Monetary Policy," Manuscript. [2391]

HAMILTON, J. D. (1994): *Time Series Analysis* (First Ed.). Princeton University Press. [2399]

HANSEN, L. P., AND T. J. SARGENT (1981): "Exact Linear Rational Expectations Models: Specification and Estimation," Federal Reserve Bank of Minneapolis Staff Report. [2399,2400]

HARMENBERG, K., AND H. H. SIEVERTSEN (2017): "The Labor-Market Origins of Cyclical Income Risk," Manuscript. [2399]

HEATHCOTE, J., K. STORESLETTEN, AND G. L. VIOLANTE (2010): "The Macroeconomic Implications of Rising Wage Inequality in the United States," *Journal of Political Economy*, 118 (4), 681–722. [2404]

HERBST, E. P., AND F. SCHORFHEIDE (2015): *Bayesian Estimation of DSGE Models*. Princeton University Press. [2394,2399,2400]

HOPENHAYN, H. A. (1992): "Entry, Exit, and Firm Dynamics in Long Run Equilibrium," *Econometrica*, 60 (5), 1127–1150. [2391]

JUDD, K. L., AND S.-M. GUU (1993): "Perturbation Solution Methods for Economic Growth Models," in *Economic and Financial Modeling With Mathematica®*, ed. by H. R. Varian. New York, NY: Springer New York, 80–103. [2397]

JUILLARD, M. (1996): "Dynare: A Program for the Resolution and Simulation of Dynamic Models With Forward Variables Through the Use of a Relaxation Algorithm," CEPREMAP Working Paper no 9602. [2404]

JUSTINIANO, A., G. E. PRIMICERI, AND A. TAMBALOTTI (2011): "Investment Shocks and the Relative Price of Investment," *Review of Economic Dynamics*, 14 (1), 102–121. [2402]

KAPLAN, G., AND G. L. VIOLANTE (2018): "Microeconomic Heterogeneity and Macroeconomic Shocks," *Journal of Economic Perspectives*, 32 (3), 167–194. [2378,2404]

KAPLAN, G., B. MOLL, AND G. L. VIOLANTE (2018): "Monetary Policy According to HANK," *American Economic Review*, 108 (3), 697–743. [2377]

KHAN, A., AND J. K. THOMAS (2008): "Idiosyncratic Shocks and the Role of Nonconvexities in Plant and Aggregate Investment Dynamics," *Econometrica*, 76 (2), 395–436. [2391]

KOBY, Y., AND C. WOLF (2020): "Aggregation in Heterogeneous-Firm Models: Theory and Measurement," Manuscript. [2404]

KRUEGER, D., AND A. LUDWIG (2007): "On the Consequences of Demographic Change for Rates of Returns to Capital, and the Distribution of Wealth and Welfare," *Journal of Monetary Economics*, 54 (1), 49–87. [2404]

KRUEGER, D., K. MITMAN, AND F. PERRI (2016): "Chapter 11—Macroeconomics and Household Heterogeneity," in *Handbook of Macroeconomics*, Vol. 2, ed. by J. B. Taylor and H. Uhlig. Elsevier, 843–921. [2378]

KRUSELL, P., AND A. A. SMITH (1998): "Income and Wealth Heterogeneity in the Macroeconomy," *Journal of Political Economy*, 106 (5), 867–896. [2377-2380,2402]

LAFFARGUE, J.-P. (1990): "Résolution D'un Modèle Macroéconomique Avec Anticipations Rationnelles," *Annales d'Économie et de Statistique*, 17, 97–119. [2404]

LORENZONI, G. (2009): "A Theory of Demand Shocks," *American Economic Review*, 99 (5), 2050–2084. [2386]

MANKIW, N. GREGORY, AND R. REIS (2007): "Sticky Information in General Equilibrium," *Journal of the European Economic Association*, 5 (2–3), 603–613. [2399]

MCKAY, A., E. NAKAMURA, AND J. STEINSSON (2016): "The Power of Forward Guidance Revisited," *American Economic Review*, 106 (10), 3133–3158. [2377]

MERTENS, T. M., AND K. L. JUDD (2018): "Solving an Incomplete Markets Model With a Large Cross-Section of Agents," *Journal of Economic Dynamics and Control*, 91, 349–368. [2378]

MEYER-GOHDE, A. (2010): "Linear Rational-Expectations Models With Lagged Expectations: A Synthetic Method," *Journal of Economic Dynamics and Control*, 34 (5), 984–1002. [2400]

MOLICO, M. (2006): "The Distribution of Money and Prices in Search Equilibrium," *International Economic Review*, 47 (3), 701–722. [2392]

PLAGBORG-MØLLER, M. (2019): "Bayesian Inference on Structural Impulse Response Functions," *Quantitative Economics*, 10 (1), 145–184. [2400]

PLAGBORG-MØLLER, M., AND L. LIU (2019): "Full-Information Estimation of Heterogeneous Agent Models Using Macro and Micro Data," Manuscript. [2399,2401]

POSTEL-VINAY, F., AND J.-M. ROBIN (2002): "Equilibrium Wage Dispersion With Worker and Employer Heterogeneity," *Econometrica*, 70 (6), 2295–2350. [2392]

PROEHL, E. (2019): "Approximating Equilibria With Ex-Post Heterogeneity and Aggregate Risk," SSRN Scholarly Paper ID 2620937, Social Science Research Network, Rochester, NY. [2378]

REITER, M. (2009): "Solving Heterogeneous-Agent Models by Projection and Perturbation," *Journal of Economic Dynamics and Control*, 33 (3), 649–665. [2375,2378,2395]

——— (2010): "Approximate and Almost-Exact Aggregation in Dynamic Stochastic Heterogeneous-Agent Models," IHS Working Paper 258. [2379,2387]

SCHMITT-GROHÉ, S., AND M. URIBE (2010): "Evaluating the Sample Likelihood of Linearized DSGE Models Without the Use of the Kalman Filter," *Economics Letters*, 109 (3), 142–143. [2399]

SIMON, H. A. (1956): "Dynamic Programming Under Uncertainty With a Quadratic Criterion Function," *Econometrica*, 24 (1), 74–81. [2397]

SMETS, F., AND R. WOUTERS (2007): "Shocks and Frictions in US Business Cycles: A Bayesian DSGE Approach," *American Economic Review*, 97 (3), 586–606. [2394,2399,2400,2402]

STRAUB, L. (2017): "Consumption, Savings, and the Distribution of Permanent Income," Manuscript. [2391, 2404]

THEIL, H. (1957): "A Note on Certainty Equivalence in Dynamic Planning," *Econometrica*, 25 (2), 346–349. [2397]

WINBERRY, T. (2018): "A Method for Solving and Estimating Heterogeneous Agent Macro Models," *Quantitative Economics*, 9 (3), 1123–1151. [2379,2401]

YOUNG, E. R. (2010): "Solving the Incomplete Markets Model With Aggregate Uncertainty Using the Krusell–Smith Algorithm and Non-Stochastic Simulations," *Journal of Economic Dynamics and Control*, 34 (1), 36–41. [2384]

Co-editor Giovanni L. Violante handled this manuscript.

Manuscript received 28 June, 2019; final version accepted 27 March, 2021; available online 19 April, 2021.